

SCALE MODEL EMP SIMULATORS

by

Eugene Frederick Oberst

A Thesis Submitted to the Faculty of the
DEPARTMENT OF ELECTRICAL ENGINEERING
In Partial Fulfillment of the Requirements
For the Degree of
MASTER OF SCIENCE
In The Graduate College
THE UNIVERSITY OF ARIZONA

1 9 7 5

STATEMENT BY AUTHOR

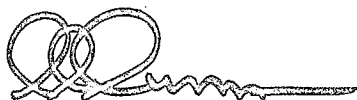
This thesis has been submitted in partial fulfillment of requirements for an advanced degree at The University of Arizona and is deposited in the University Library to be made available to borrowers under rules of the Library.

Brief quotations from this thesis are allowable without special permission, provided that accurate acknowledgment of source is made. Requests for permission for extended quotation from or reproduction of this manuscript in whole or in part may be granted by the head of the major department or the Dean of the Graduate College when in his judgment the proposed use of the material is in the interests of scholarship. In all other instances, however, permission must be obtained from the author.

SIGNED: Eugene F. Oberst

APPROVAL BY THESIS DIRECTOR

This thesis has been approved on the date shown below:



Donald G. Dudley
Professor of Electrical Engineering

10/17/74
Date

ACKNOWLEDGMENTS

I would like to take this opportunity to express my appreciation to my professors and associates for their assistance in the accomplishment of this study. A special thanks goes to Dr. Donald G. Dudley for his guidance and technical assistance throughout all phases of this work. A special thanks also goes to my friends and associates, David Seidel, Jeffery Beren and Dr. Clyde Dease for their moral and technical support in this task. Without the aid of these people, it would not have been possible to complete this work in such a relatively short period of time.

I would also like to express my appreciation to my wife and children for their patience and understanding during the past five years. Without their help, none of this would have been possible.

Finally, I would like to thank Mrs. Freida Long for her assistance in the final preparation of this thesis. Her knowledge and experience in such matters were invaluable.

TABLE OF CONTENTS

	Page
LIST OF ILLUSTRATIONS	vi
LIST OF TABLES	ix
ABSTRACT	x
 CHAPTER	
1 INTRODUCTION	1
2 FABRICATION AND TESTING OF A 1/40 SCALE MODEL COMMERCIAL COMMUNICATIONS STATION WITH TOWER AND GUY WIRES	3
Theory of Electromagnetic Scaling	3
Construction of Test Facility	4
Ground Plane	4
Communications Center Model	10
EMP Source	12
Measurement System	18
Tests	25
Measurement System Tests	25
EMP Source Tests	29
Data Repeatability Test	41
Performance Evaluation	45
3 FABRICATION AND TESTING OF A 1/20 SCALE MODEL PARALLEL PLATE EMP SIMULATOR	46
Construction of Test Facility	46
Ground Plane	46
Parallel Plate Structure	46
EMP Source	50
Measurement System	55
Tests	58
Measurement System Tests	58
EMP Source Tests	67

TABLE OF CONTENTS (Continued)

	Page
Cross-Polarized E-Field Component Test	70
Performance Evaluation	75
4 CONCLUSIONS	79
LIST OF REFERENCES	80

LIST OF ILLUSTRATIONS

Figure		Page
2.1	Ground Plane	6
2.2	Test Facility	7
2.3	Test Facility with Model Area in Place	8
2.4	Test Facility with Model Area Removed	9
2.5	Model Area Access	11
2.6	Model Area	13
2.7	EMP Source Block Diagram	14
2.8	Pulse Shaping Network	16
2.9	Source Monopole Mount Assembly	17
2.10	Model Building with H-Field Sensors Installed	19
2.11	Source Monopole	20
2.12	Measurement System Block Diagram	21
2.13	H-Field Sensors	23
2.14	H-Field Sensor Unit	24
2.15	E-Field Probe Mount	26
2.16	H-Field Sensor Output	27
2.17	Ray Paths for Analyzing Sensor Output	31
2.18	Tower Reflection Signal	33
2.19	Estimated Sensor Response	35
2.20	Refined Reflected Signal from Model Tower	37
2.21	Refined Estimated Sensor Response	38

LIST OF ILLUSTRATIONS (Continued)

Figure	Page
2.22 Incident Pulse Peak Amplitude (Normalized) as a Function of $1/R$	40
2.23 Comparison of Pulse Generator Output with Radiated Pulse	42
2.24 Repeatability Test Data #1	43
2.25 Repeatability Test Data #2	44
3.1 Model EMP Simulator	47
3.2 Model Dimensions	49
3.3 EMP Source Block Diagram	51
3.4 Pulse Generating Circuit	53
3.5 TEM Horn	54
3.6 Test Point Locations	57
3.7 Block Diagram of Integrating and Recording Setup	59
3.8 Square Wave Input to Integrator	62
3.9 Integrator Output with Square Wave Input	63
3.10 Short Monopole Response to Double Exponential Pulse Input	64
3.11 Integrated Short Monopole Response to Double Exponential Pulse Input	65
3.12 Graphically Integrated Short Monopole Response to Double Exponential Pulse Input	66
3.13 Integrated Response from Reference E-Field Probe	68
3.14 Non-Integrated Response from Reference E-Field Probe	69
3.15 Reflection Coefficient for Twin Lead to TEM Horn Connection	71

LIST OF ILLUSTRATIONS (Continued)

Figure		Page
3.16	E-Field Configurations for Parallel Plate Guides	72
3.17	E-Field Configuration for a Finite Parallel Plate Structure in the Vicinity of a Ground Plane	74
3.18	Integrated Response of E-Field Sensor at Test Point #1 .	76
3.19	Integrated Response of E-Field Sensor at Test Point #4 .	77
3.20	Integrated Response of E-Field Sensor at Test Point #6 .	78

LIST OF TABLES

Table		Page
2.1	Distance and Time Differences for Various Ray Paths . . .	32
2.2	Amplitude Factors	36

ABSTRACT

This thesis describes two simulators which were developed to provide an experimental approximation to the electromagnetic pulse (EMP) environment which exists during a nuclear explosion.

The simulators were subjected to tests which would determine how well they reproduced the EMP environment. The results of this testing indicate that while one of the simulators produced all of the desired conditions, the other simulator had a serious design deficiency which negated its usefulness as an EMP simulator.

In both cases, however, the information obtained from these two simulators indicate that scale model EMP simulators are useful tools in the study of electromagnetics.

CHAPTER 1

INTRODUCTION

With the advent of nuclear weapons, much time has been spent studying the threat potentials of these devices from both offensive and defensive viewpoints. Initially, the primary concern was with the threat potentials of blast and radioactive fallout. In recent years these studies have been broadened to include other areas of potential threat such as that associated with the electromagnetic pulse (EMP) generated during a nuclear explosion.

Since it was not practical to pursue these studies only during a nuclear explosion, devices had to be developed which could simulate the EMP environment. These devices, referred to as EMP simulators, have been built in a variety of ways. The objective of this thesis is to describe some of the techniques used in the design and construction of two scale model EMP simulators, which were built at The University of Arizona, and to discuss the results of tests performed to determine the capability of the simulators to produce the desired conditions.

The first simulator to be discussed was built to study the effects of guy wire coupling of an EMP to a model communications center [Dudley and Oberst, 1974]. The model to be used was a 1/40 scale communications installation consisting of an electronic equipment building, a microwave tower, and guy wires for the tower. Various guy wire configurations were to be considered. The EMP signal to be used for the tests

was to be of the double exponential type with a rise time scaled from less than 30 NS and a fall time scaled from greater than 150 NS. The radiated wave would be vertically polarized and would have a grazing angle of incidence.

The second simulator to be discussed was constructed to study a proposed design for a full scale EMP simulator [Dudley, 1974]. The basic idea for the simulator was a parallel plate structure which would be tilted at an angle of 25-30 degrees, with respect to horizontal, and would intersect a ground plane. The reason for tilting the structure was to provide data for study from an angle of incidence other than 90° , with respect to horizontal. The region between the plates at their intersection with the ground plane would contain the working volume in which various objects would be placed for test purposes. The simulator would also have a matched load connected to it so that reflections from the ground plane, in the region between the plates where they intersect the ground plane, would be absorbed. The simulator would theoretically produce a horizontally polarized TEM wave. The pulse to be used in the full scale simulator would be a double exponential type with a rise time of less than 15 NS and a fall time ($1/e$) of greater than 120 NS. The scale model version of the simulator was to be built on a 20:1 scale reduction.

CHAPTER 2

FABRICATION AND TESTING OF A 1/40 SCALE MODEL COMMERCIAL COMMUNICATIONS STATION WITH TOWER AND GUY WIRES

Theory of Electromagnetic Scaling

The principles of electromagnetic scaling have long been used by antenna design engineers in cases where an antenna design could not be tested under the same conditions in which it was to be used, either because of size or environmental limitations. In designing a scale model, conditions for exact simulation are satisfied if the following requirements are met [Weeks, 1968]:

1. The linear dimensions of the model are $1/n$ times the full scale device.
2. The operating frequency and conductivity of the materials used in the model are n times those of the full scale device.
3. The complex electric permittivity and magnetic permeability of the materials used in the model are the same as in the full scale device.

The value of the scale factor, n , is chosen such that the three conditions given are satisfied. Of the three, the condition concerning frequency is the hardest to satisfy for the pulse specifications given. Studies have shown [E-H Research Labs., Inc., 1968] that the rise time of a pulse is inversely proportional to the high frequency content of

the pulse. Thus, to satisfy the higher frequency requirement the rise time of the scaled pulse must be $1/n$ times the full scale value. Pulse rise times are essentially determined by the capabilities of the pulse generator and the limitations imposed by the measurement system. Both of these factors are controllable through the design and construction of these items. It was with this fact in mind that the design and construction of the scale model simulators was carried out.

Construction of Test Facility

Ground Plane

The ground plane is 8.54 mtrs. square and is made of aluminum screen stretched over a wooden frame. The structure was erected on the roof of a building and has a .914 mtr. space between the framework and the roof. This allows underneath access to the center portions of the ground plane without having to walk on its surface. The wooden framework of the ground plane was designed to provide sufficient support for the screen material, and thus keep the ripples to an acceptable level, and at the same time keep the weight of the structure to a minimum. The 1.22 mtr. wide strips of screen were overlapped and stapled to provide a continuous surface.

The locations of the EMP source antenna and the center of the model area were selected to provide the maximum separation between them and at the same time give the longest possible clear time to the edges of the ground plane.

The model area is a 1.372 mtr. diameter sheet metal plate backed with a 1.22 mtr. diameter 1.27 cm. plywood sheet. The supporting

structure for the model area is made from two 1.22 x 2.44 mtrs. x 1.27 cm. sheets of plywood with a hole of slightly larger than 1.22 mtr. diameter. This allows the sheet metal plate to sit flush on the screen covering. A thin strip of rubber was placed around the hole, under the screen covering, to insure that the metal plate would be in contact with the screen at all points. This arrangement for the model area allows it to be rotated from underneath a full 360°, and thereby simulates changing the location of the EMP source with respect to the structures mounted on the plate.

Grounded tie points for the guy wires on the model tower were provided for by mounting small brass plates every 15° around a circle of 1.372 mtrs. radius from the center of the model area. The guy wires are fed through small holes in the brass plates and are secured beneath the ground plane. When the position of the model area is to be changed, the guy wires are released and reinserted in another brass plate at the location corresponding to the new position of the model area. Since tie points are provided at 15° intervals, the position of the model can be changed in increments of 15°. The underside of the support structure for the model area plate has markings corresponding to 15° intervals so that the plate may be positioned without difficulty.

Figure 2.1 gives the general structure and layout of the ground plane. It was necessary to cut out two of the corners as shown because of other structures in the area. This does not reduce the clear time to the edges however. Figures 2.2 and 2.3 are photographs of the test facility taken from different angles. Figure 2.4 shows how the model

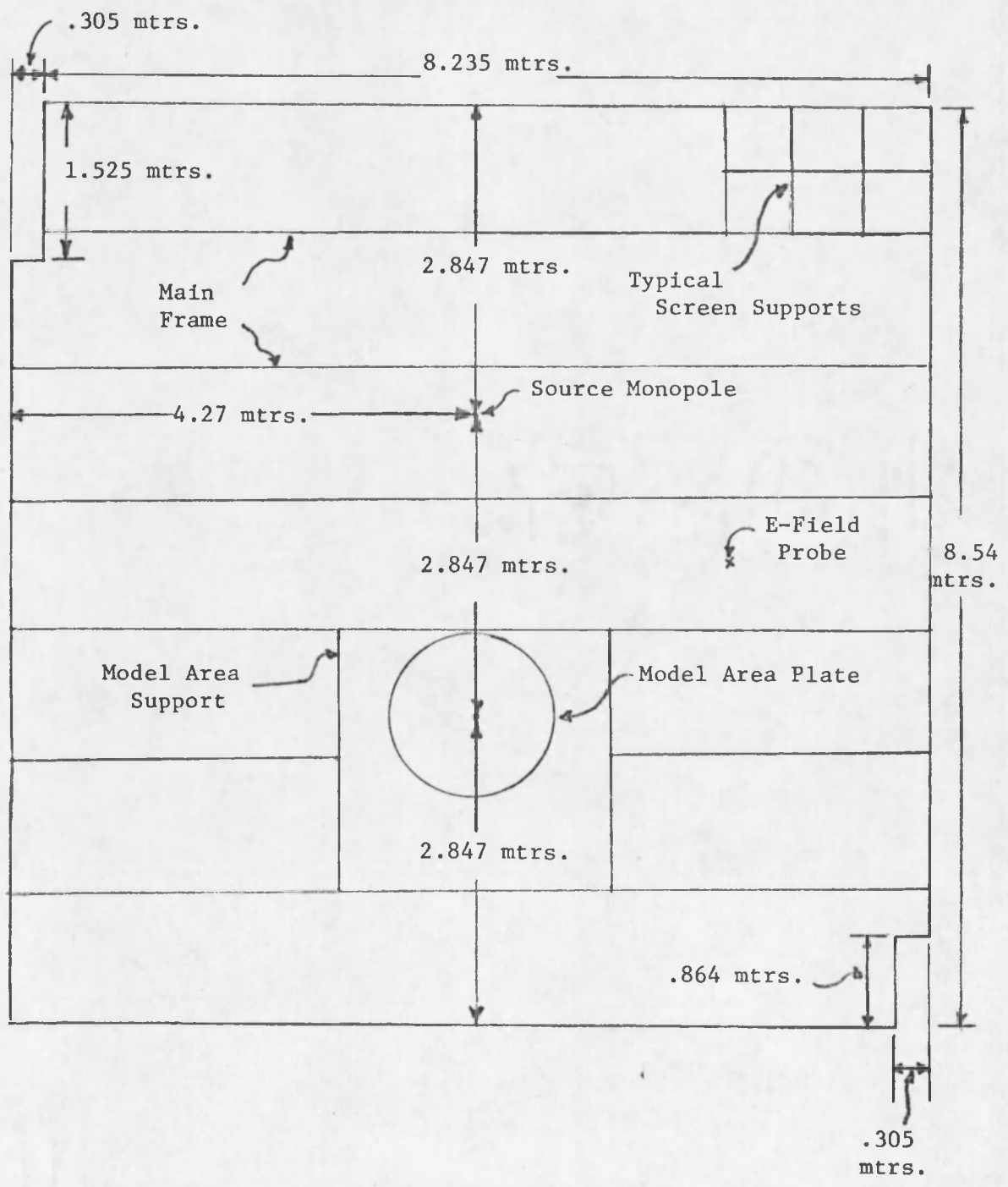


Fig. 2.1 Ground Plane



Fig. 2.2 Test Facility



Fig. 2.3 Test Facility with Model Area in Place



Fig. 2.4 Test Facility with Model Area Removed

area may be removed. Figure 2.5 shows how access to the model area is gained.

Communications Center Model

The model communications center consists of an electronic equipment building, a microwave tower and guy wires associated with the tower. The dimensions of the structures and the distance between various points were based on an average value of the figures given for the full scale facilities. The microwave tower is located in the center of the model area. The location of the building and the ground tie points for the guy wires are referenced to the tower.

Because of the frequency content of the source pulse, both the building and tower structures have been simplified. The spacing between the reinforcing bars of the walls of the electronics building is assumed small enough to be modeled by a solid piece of sheet metal. Likewise, the actual tower structure is triangular in shape, with a tapered base, and has vertical steel members with crisscrossing braces. This complicated structure was simply modeled using a solid copper pipe neglecting the edges of the triangular tower and the space between the braces. The tapered section at the base has been neglected since it represents a small percentage of the overall height of the tower. Since the study is primarily concerned with the coupling effects of the guy wires on the tower and is comparative in nature, it was felt that these simplifications of the model structures would not significantly affect the test results.

The model building is 76.2 cm. x 38.1 cm. x 11.43 cm. and has facilities for the mounting of H-field sensors on all walls and the roof.



Fig. 2.5 Model Area Access

Access to the sensors is through a hole in the plate beneath the building.

The tower protrudes through the model area plate a distance of 1.52 mtrs. above the ground plane and is held in place by a clamp on the underside of the plate. A small metal collar around the tower at its base assures electrical contact with the ground plane. Small eyelets were soldered to the tower to provide tie points for the guy wires.

The guy wires are made from No. 22 uncoated copper wire. Some portions of the tests require that the guy wires be insulated from the tower. For these cases, short pieces of teflon insulation are placed around the wires at the tower tie points.

Since the tower is free to rotate independently from the model area plate, different guy wire orientations with respect to the model building can be obtained.

Figure 2.6 shows the general layout of the model area with the guy wires in one of the configurations chosen to be tested.

EMP Source

The EMP source consists of a high voltage DC power supply, a pulse generator, a 2.74 mtr. vertical monopole and an interconnecting signal cable. Figure 2.7 is a block diagram of the source.

The DC power supply is a Polytechnic type 812 klystron power supply. The beam voltage output of this unit is used in the generation of the high voltage pulse. It is connected to the pulse generator through a section of RG-8/u coaxial cable.

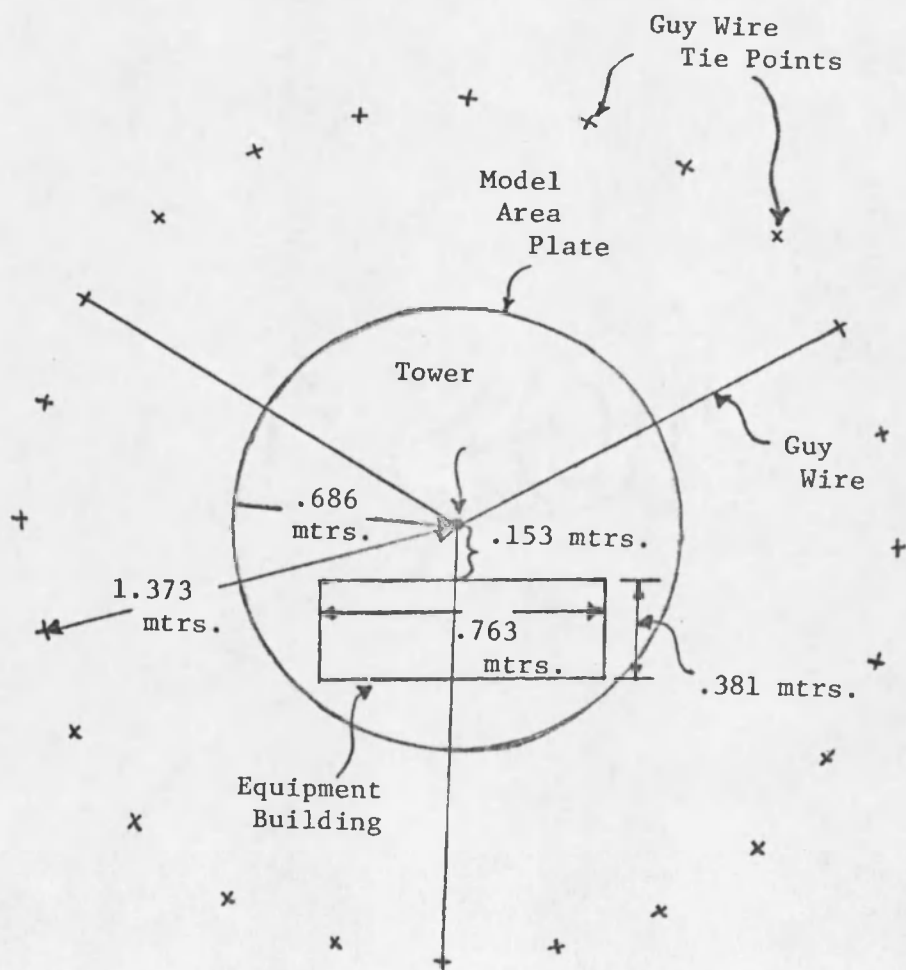


Fig. 2.6 Model Area

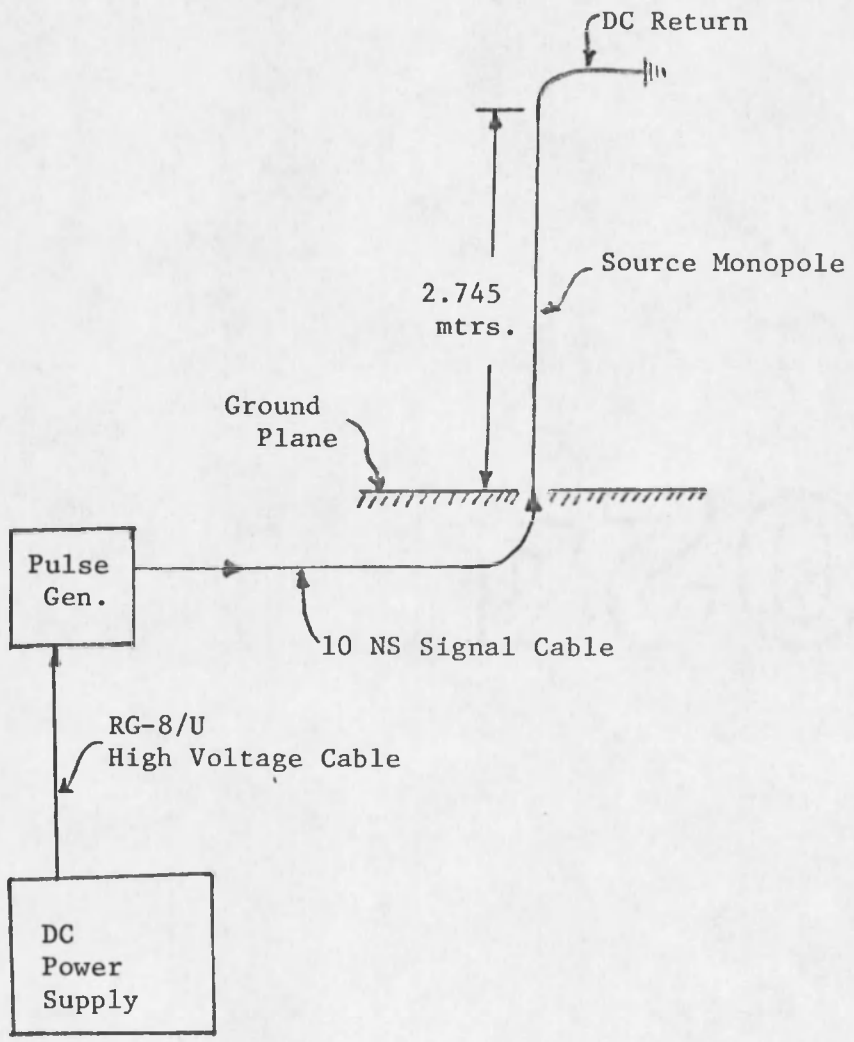


Fig. 2.7 EMP Source Block Diagram

The pulse generator was designed and built by students at The University of Arizona. The unit is self-contained except for the high voltage DC power supply used for the pulse. It has the capability of producing several pulse shapes of variable duration and repetition rate. For this project, the unit produces a double exponential type pulse with rise time of approximately 700 PS and a fall time (one over e time) of approximately 6.5 NS. The pulse is generated by discharging a capacitor through a mercury-wetted reed switch (Fig. 2.8) into the load resistance. The switch, capacitor, and a current limiting resistor are all mounted inside a General Radio type 874-X insertion unit. The capacitor is connected as close as possible to the switch to prevent reflection from distorting the pulse. The switch is energized by a coil wound around the outer shield of the insertion unit. The peak amplitude of the output pulse is approximately 1.4 KV and a pulse repetition rate of 200 PPS was used.

The monopole is a length of .635 cm. aluminum rod that protrudes 2.74 mtrs. above the ground plane. It is tapped on one end to allow it to be fastened to a transition stage between the signal cable and the surface of the ground plane (Fig. 2.9). The transition stage provides an easy method of connecting the signal cable to the antenna, a firm base for the antenna to set on, and maintains the same characteristic impedance as the signal cable up to the surface of the ground plane. The other end of the monopole is threaded to allow it to be attached to a support structure above the ground plane. Since the monopole is flexible, the support structure was necessary to maintain the antenna

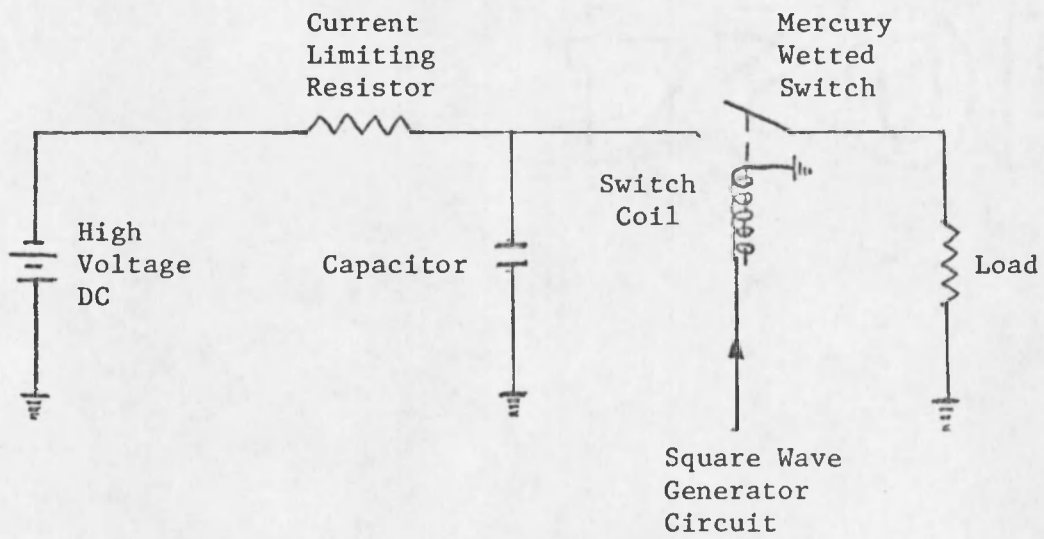


Fig. 2.8 Pulse Shaping Network

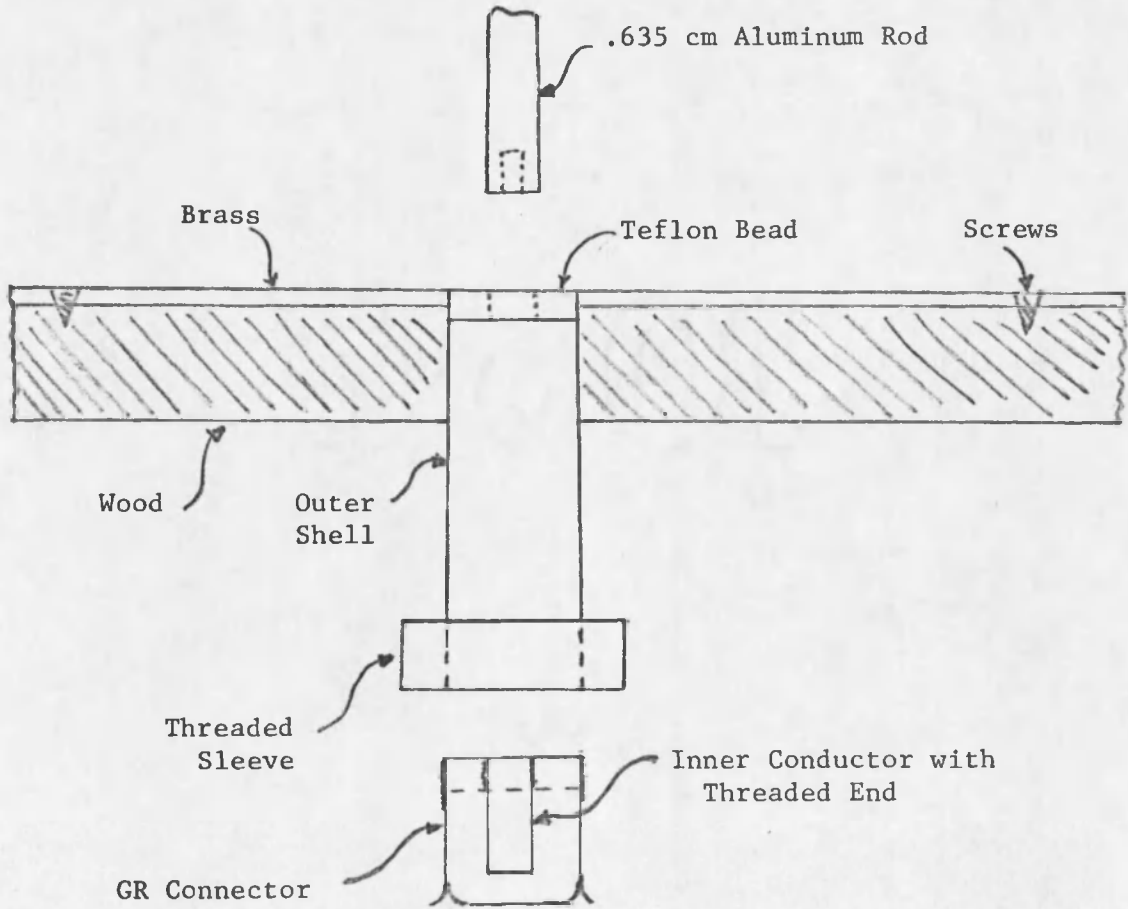


Fig. 2.9 Source Monopole Mount Assembly

in a vertical position at all times. A DC return path is provided for by a wire connected between the top of the monopole and the ground plane. The characteristic impedance of this wire is not much different from that of the monopole and, therefore, very little reflection occurs at this point.

Since the monopole is longer than the duration of the pulse, the pulse is transmitted without distortion caused by reflections from opposite ends of the antenna. The main radiation is at the base of the monopole and is spherical in nature [Schmitt, Harrison and Williams, 1966]. It was assumed that by the time the wave front reaches the model area that it is a good approximation of a plane wave. (See EMP Source Tests Section.)

The signal cable that connects the pulse generator to the monopole is a piece of low loss coaxial cable. Its length is approximately 10 NS, which provides a 20 NS delay between the initial wave front and the wave front created by the energy reflected back to the pulse generated from the base of the monopole.

Figure 2.10 is a view of the model building which shows the H-field sensors mounted in two of the walls and the roof. Figure 2.11 shows the source monopole and its mounting plate.

Measurement System

The measurement system (Fig. 2.12) consists of a Tektronics type 567 readout oscilloscope, with type 6R1A digital unit, type 3T77 sampling sweep and type 3S76 sampling dual trace plug-in units, a Polaroid CR-9 land camera, H-field sensors, and a 12 cm reference and trigger pulse E-field probe.

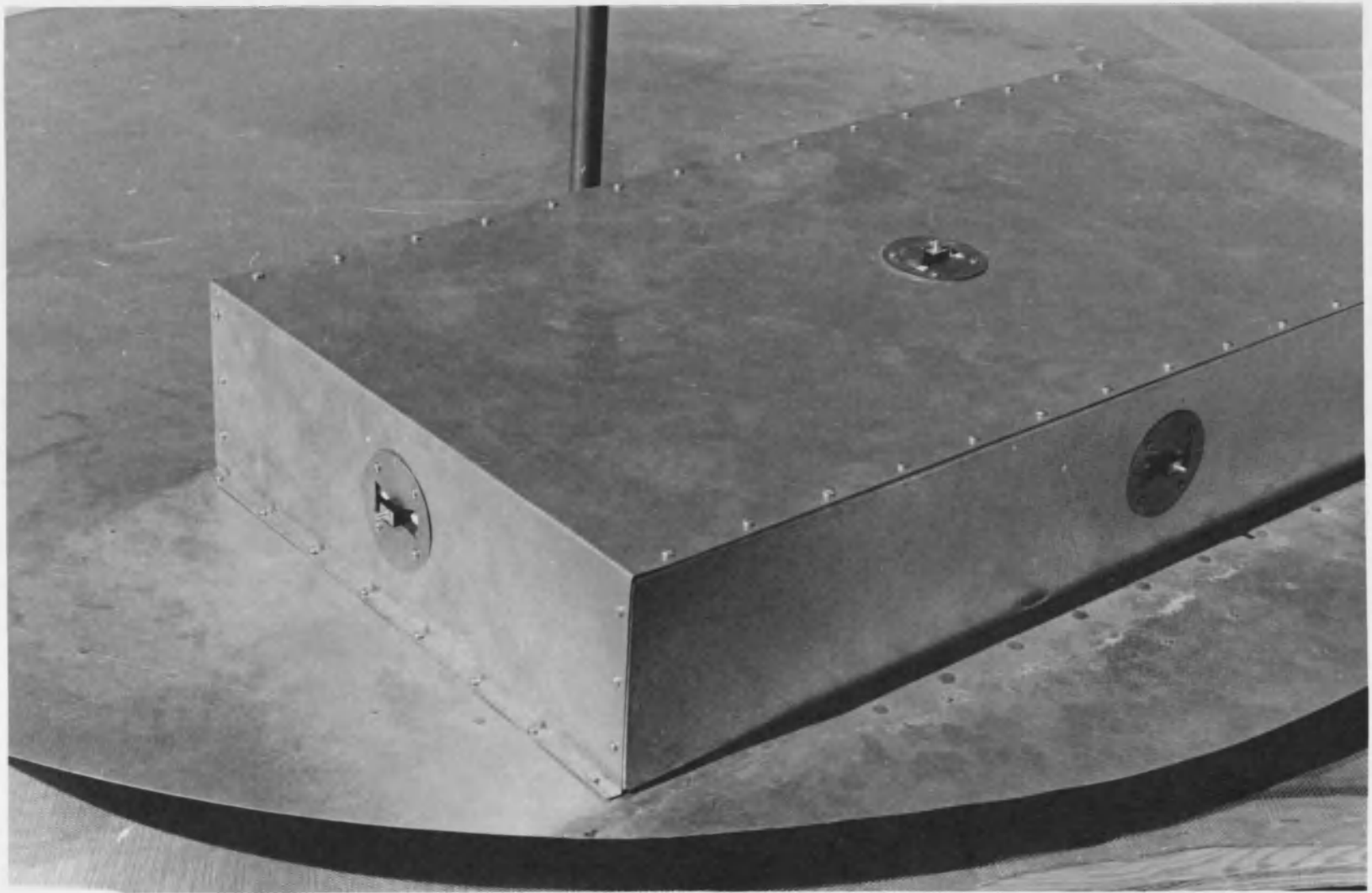


Fig. 2.10 Model Building with H-Field Sensors Installed



Fig. 2.11 Source Monopole

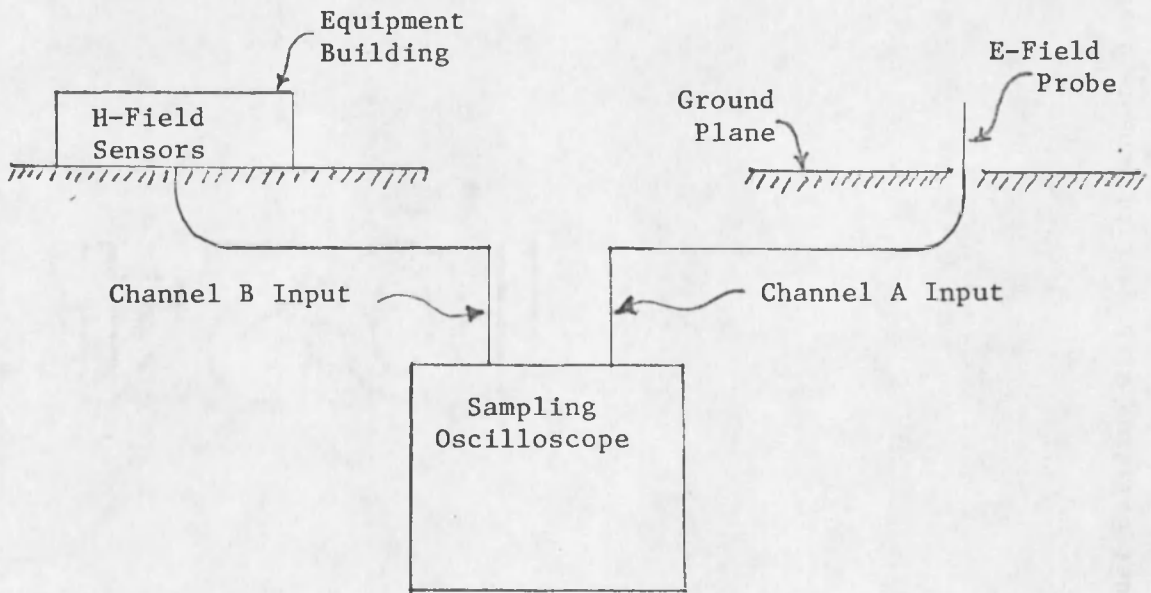


Fig. 2.12 Measurement System Block Diagram

The oscilloscope, with the above mentioned plug-in units, has a rise time of 400 PS, 50 ohm input impedance, 2 MV (peak-to-peak) normal noise and uses a sampling process to produce high resolution without jitter.

Although the oscilloscope has recorder outputs, it was decided to photograph the measured data because of external noise interference with the recorder's operation. The camera used has the capability of manually timing the exposure which, when coupled with the oscilloscope's single display feature, produces a good resolution picture of the data.

The H-field sensors (Fig. 2.13) are actually made up of two components, a short circuited slot and a current transformer to measure the short circuit current. This current corresponds to the tangential magnetic field on the sensor. The units were designed by Stanford Research Institute and consist of a 6.34 cm. diameter brass outer plate with a slot, a 6.35 cm. diameter inner retaining ring and associated mounting hardware (Fig. 2.14). To use the unit, a 5.08 cm. diameter hole is cut in the metal surface of the model. The metal surface is then clamped between the outer plate and the inner retaining ring using the mounting hardware. The position of the sensor can be changed by loosening the mounting hardware and rotating the entire unit. Since the slot is a directional device, rotation of it permits measurement of orthogonal components of the magnetic fields. The slot is 4 cm. long and .952 cm. wide in the middle to allow for mounting the current transformer. The ends of the slot are tapered out to 1.91 cm. which gives the slot a wider bandwidth.

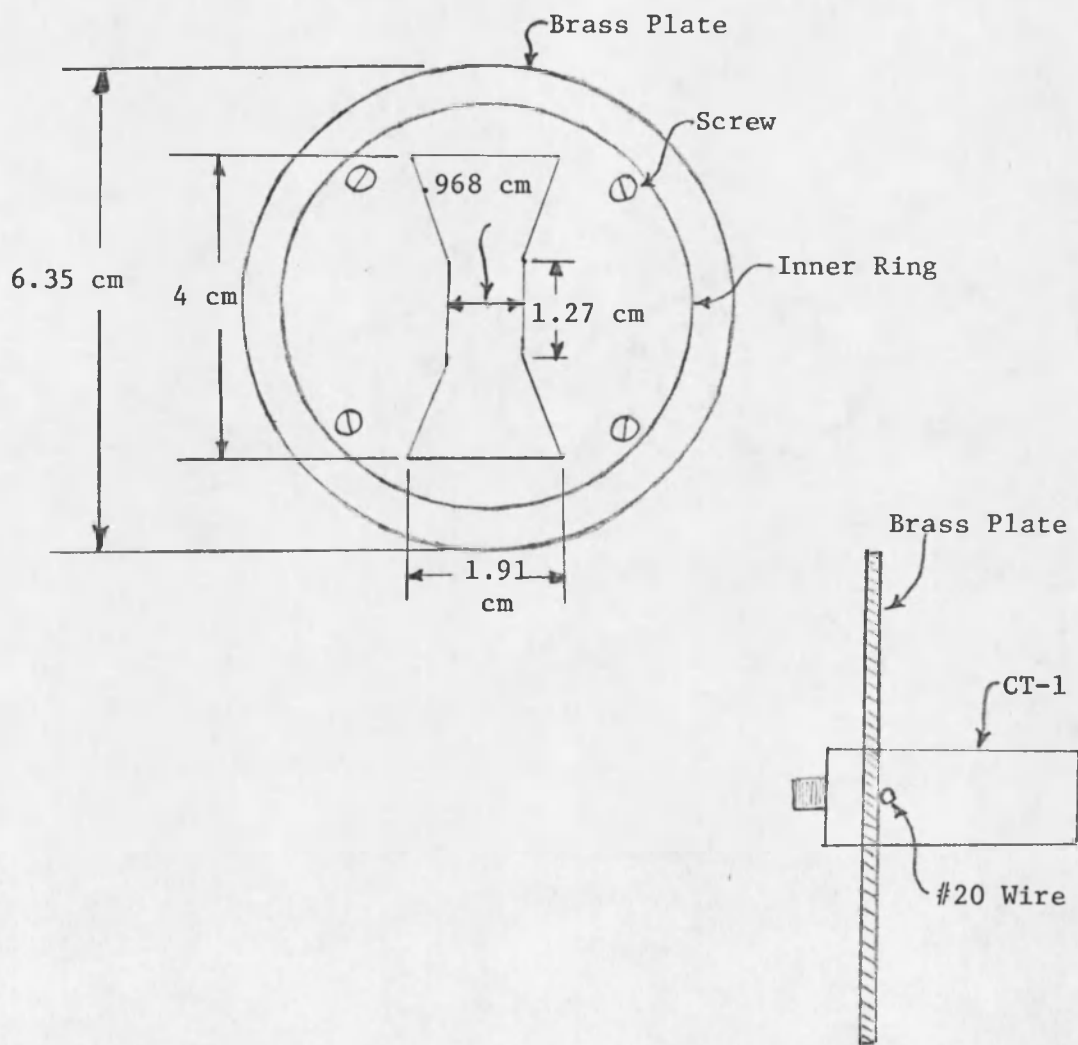


Fig. 2.13 H-Field Sensors

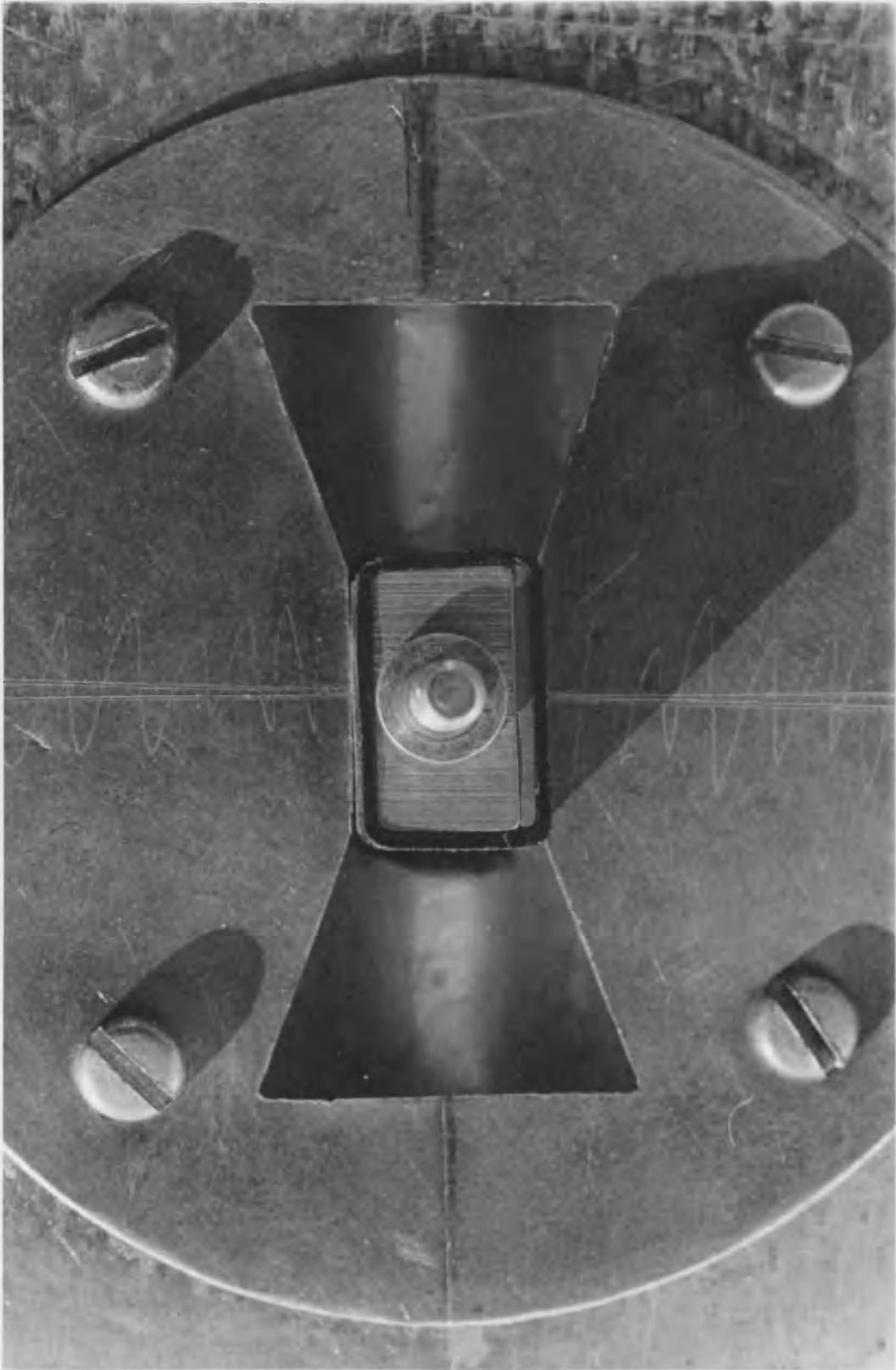


Fig. 2.14 H-Field Sensor Unit

The current transformer used is a Tektronix type CT-1. It has a sensitivity of 5 MV/MA into a 50 ohm load, a rise time of less than 350 PS, low frequency limit of 35 K Hz (3 db point) and a decay of less than 1% over the first 50 NS. The insertion impedance with a 50 ohm termination is 1 ohm shunted by 5 uh.

When the CT-1 is used in the H-field sensors, the transformer loads the slot inductance such that the decay time of the sensor unit is about 13 to 14 NS. Since this is slower than the decay time of the radiated pulse, the decay can be neglected. The rise time of the total sensor unit is approximately 500 PS.

The CT-1 is connected to a Tektronix type P6040 cable. The cable is .458 mtrs. long, provides a 2.4 NS delay, and has a rise time of less than 200 PS. This cable is then connected to a low loss signal cable which feeds the data to the sampling oscilloscope.

The 12 cm. E-field probe is a vertical monopole made from No. 16 copper wire mounted in a BNC panel mount connector. The BNC connector is soldered to a small brass plate in such a manner that the threaded end is flush with the surface of the brass plate (Fig. 2.15). This probe is used to verify that the pulse being transmitted remains the same throughout the test phase. It is also used as a triggering signal for the sampling oscilloscope.

Tests

Measurement System Tests

Tests were performed on the measurement system to determine whether the level of noise in the system was acceptable, the outputs

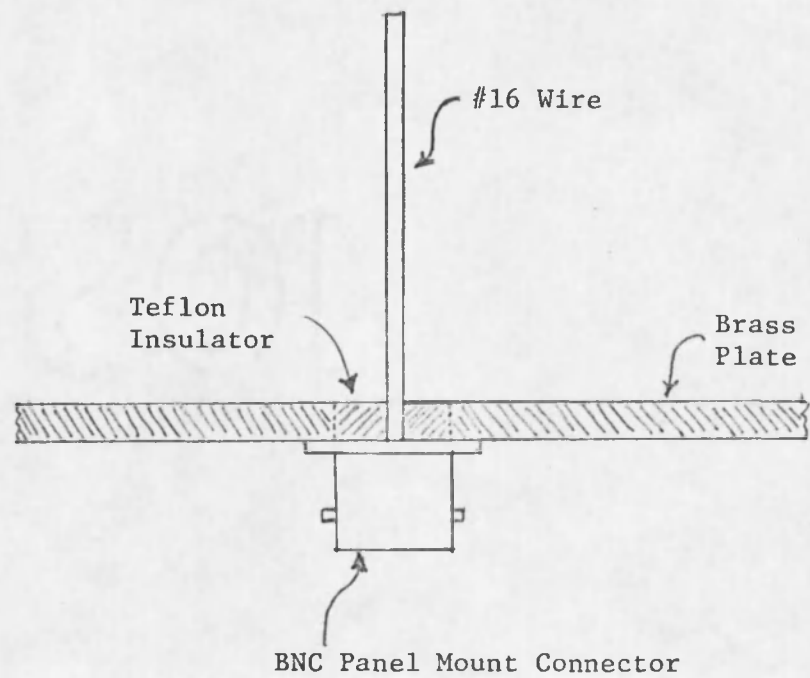
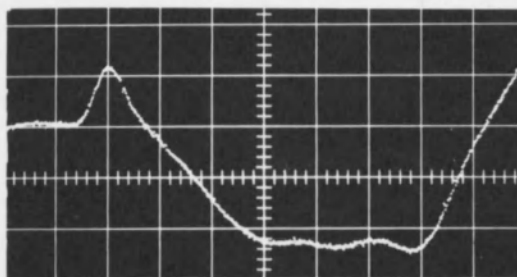


Fig. 2.15 E-Field Probe Mount



Horizontal Scale - 1 NS Div

Fig. 2.16 H-Field Sensor Output

from the H-field sensors were the same and the presentation on the sampling scope represented the initial response of the sensor to the incident wave.

The initial noise level tests showed that a large amount of noise was being admitted into the system primarily because of a lack of adequate shielding of the sampling oscilloscope. After several tests, it was found that the noise level could be kept to a minimum if the oscilloscope was placed beneath the ground plane in the vicinity of the model area. Although there are more elegant solutions to this problem, for the sake of the schedule it was decided that this solution would suffice.

The H-field sensors were checked for standardization of response to identical H-field excitation by mounting them in the same location on the model building and comparing their outputs. All of the sensors had very similar responses with the major differences being some small variations in amplitude. If it became necessary, these differences could be compensated for by a correction factor which would normalize all the sensor response amplitudes to the same value.

Since the sampling oscilloscope was not being triggered by the signals from the H-field sensors, care had to be taken to insure that the signals observed from the H-field sensors were their initial response to the incident wave. An analysis of how the sampling scope displays information was used to show that the data taken was in fact the initial response from the H-field sensors.

The sampling scope holds off displaying the triggering pulse for a period of 16.4 NS after the trace has started. Therefore, in order to

view the initial response of the sensors, the transit time for signals from the sensors can not be less than 16.4 NS shorter than the transit time for the triggering pulse. The closest time from the source for the H-field sensors is 7.7 NS, while the E-field probe remains at a constant 9.44 NS. The sensor is therefore 1.74 NS closer, at this point, to the source. The signal cable for the H-field sensor is 11.8 NS shorter than the cable from the E-field probe. Therefore, the earliest possible signal arrival time at the scope for the H-field sensors is 13.54 NS before the triggering pulse can appear at the scope or 2.86 NS after the trace has started. Thus, the data taken represents the initial response of the H-field sensors to the incident wave.

EMP Source Tests

The EMP source was tested to determine such things as the planarity of the incident wave in the vicinity of the model area and the distance dependence of the incident wave amplitude. It was also tested to determine the fidelity of the source output as compared to the pulse output of the pulse generator.

It was stated earlier that the incident wave in the vicinity of the model area was assumed to be a good approximation of a plane wave. While this is a true statement for small horizontal and vertical variations, it is not true in general.

An analysis of some of the data taken shows that for large vertical variations, there is a considerable difference in the phase of the wavefront. In particular, the data taken from one of the sensors (Fig. 2.16) was analyzed to show that this was the case.

After reviewing the data, it was decided that the model tower was the major cause for the radical difference in the response from this sensor when compared to the responses of other sensors on the model building. This difference in response can be explained by looking at the reflected signals coming from the tower.

Using a ray path technique, it was found that from the base of the source monopole there is a difference of 38.35 cm. between the path to the base of the tower and the path to the top of the tower (see Fig. 2.17). In addition, the ray path for the reflected signal is 1.38 mtrs. longer from the top of the tower to the sensor location than the reflected path from the base of the tower. The total difference in path length is thus 1.764 cm. and corresponds to a time difference of 5.87 NS between the arrival times at sensor for signals travelling along these two ray paths. Table 2.1 shows the total difference in distance for paths that intersect the tower at various heights and the corresponding time delays.

A tower reflection signal was formed by graphically adding six incident pulses, each shifted by the amount of time corresponding to ray paths indicated in Table 2.1. The resultant composite reflection signal is shown in Fig. 2.18. This signal was scaled and inverted and then graphically added to an incident pulse. The inversion is necessary because the reflected signals from the tower will have a polarity opposite to the incident pulse. The scaling was determined by matching amplitudes of the reflected and incident signals at the time corresponding to the zero crossover point for the actual response from the sensor. The

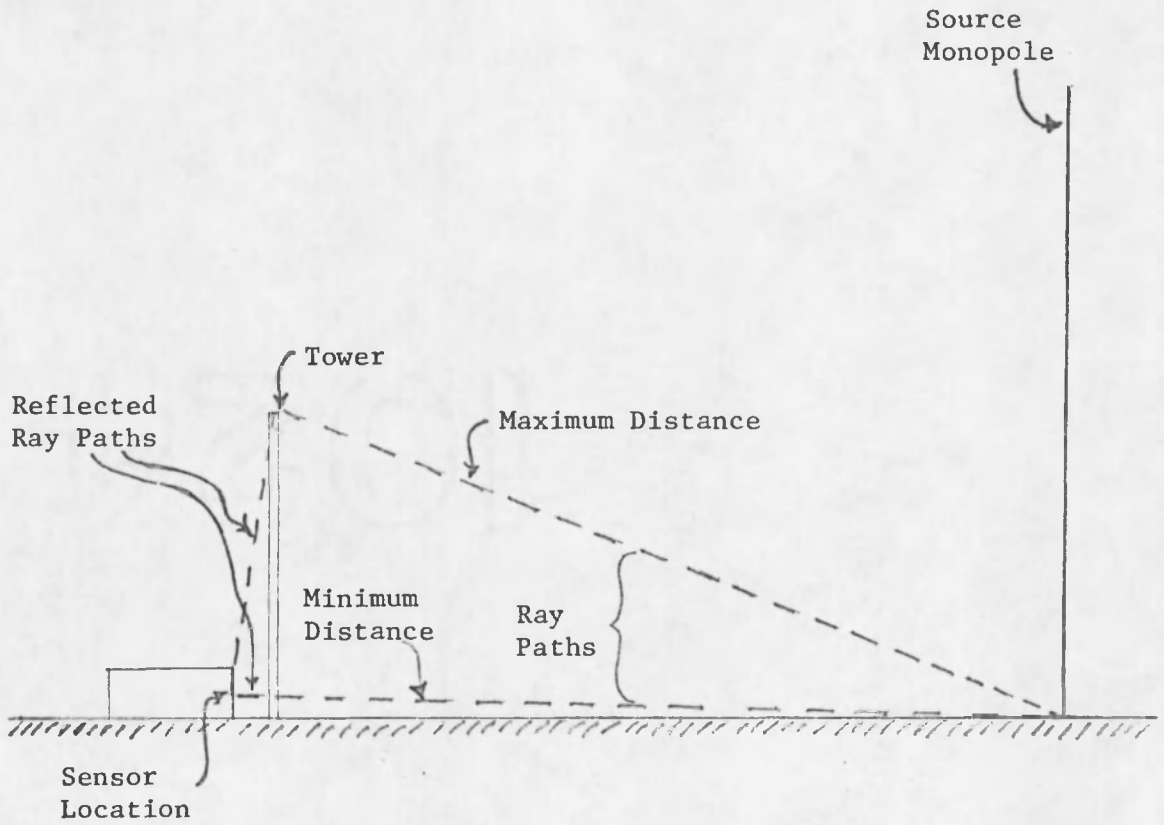


Fig. 2.17 Ray Paths for Analyzing Sensor Output

Table 2.1 Distance and Time Differences for Various Ray Paths

Ray Path	Tower Height (mtrs.)	Distance Difference (mtrs.)	Time Delay (NS)
1	0	0	0
2	.305	.205	.68
3	.610	.541	1.08
4	.915	.919	3.06
5	1.220	1.327	4.42
6	1.525	1.763	5.87

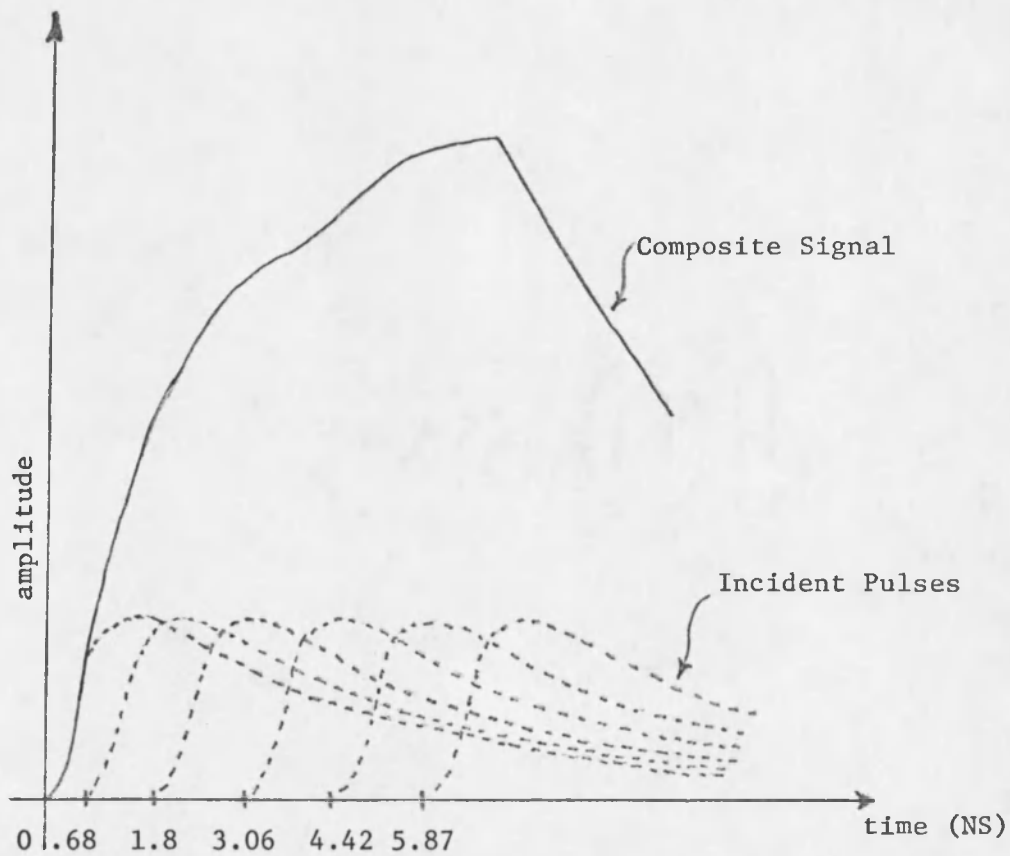


Fig. 2.18 Tower Reflection Signal

resultant composite signal is shown in Fig. 2.19. A comparison of this figure with Fig. 2.16 shows a promising similarity.

An even better result was obtained by using an inverse distance factor to adjust the amplitudes of the pulses being reflected from the tower. Since the field strength is inversely proportional to the distance traveled, far field assumed, the amplitudes of the reflected pulses must be reduced proportionally to the extra distance traveled by each one. These amplitude factors are given in Table 2.2. Taking these factors into consideration, a refined composite reflection signal was graphically produced and is shown in Fig. 2.20. Again, this signal was inverted, scaled, and graphically added to an incident pulse. The result is shown in Fig. 2.21.

A comparison between this signal and the actual response from the sensor shows that they are almost identical from the first 4 NS. The difference between the two beyond this point is probably caused by reflections from the model building edges and the guy wires. However, it can be seen from the results obtained by this analysis that the wavefront is not planar over a large distance.

For small variations in vertical height, the wavefront can be considered planar. As an example, wavefront arrival time variations over the height of the model building walls amounts to a difference of 7.26 PS between the bottom and the top of the wall. Lateral variations along the widest dimension of the building amount to a difference of 80.4 PS in wavefront arrival time between the center of the wall and either end. For the ranges used in taking the data, these time variations are undistinguishable.

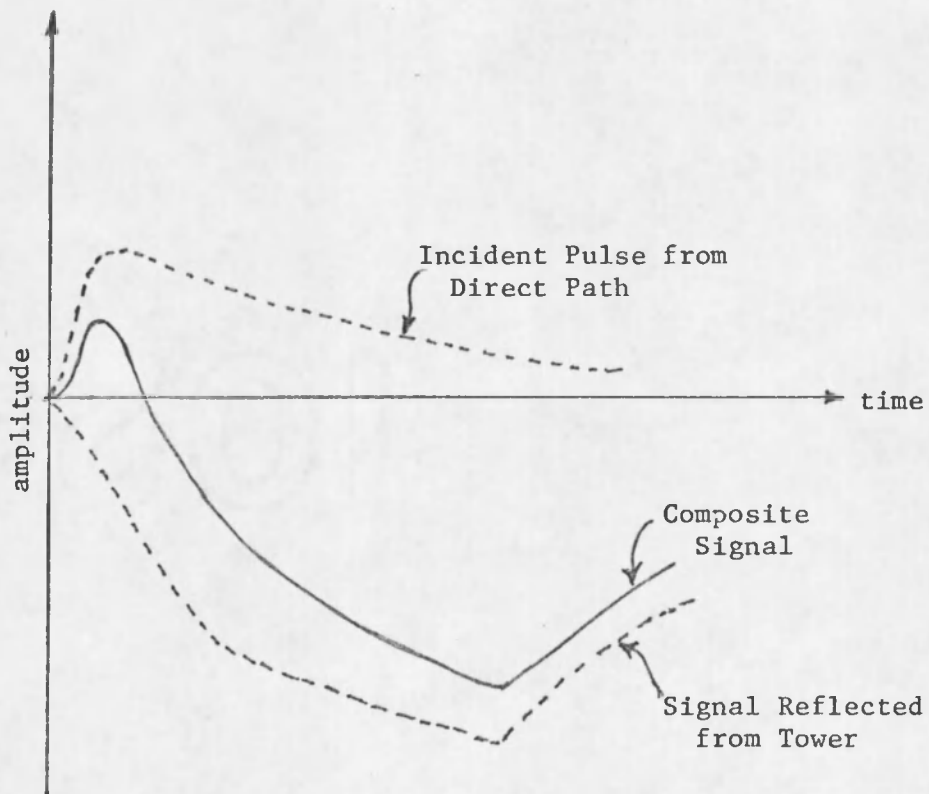


Fig. 2.19 Estimated Sensor Response

Table 2.2 Amplitude Factors

Ray Path	Distance (mtrs.)	Amplitude Factor
1	2.999	1.000
2	3.204	.936
3	3.540	.847
4	3.918	.766
5	4.326	.693
6	4.762	.630

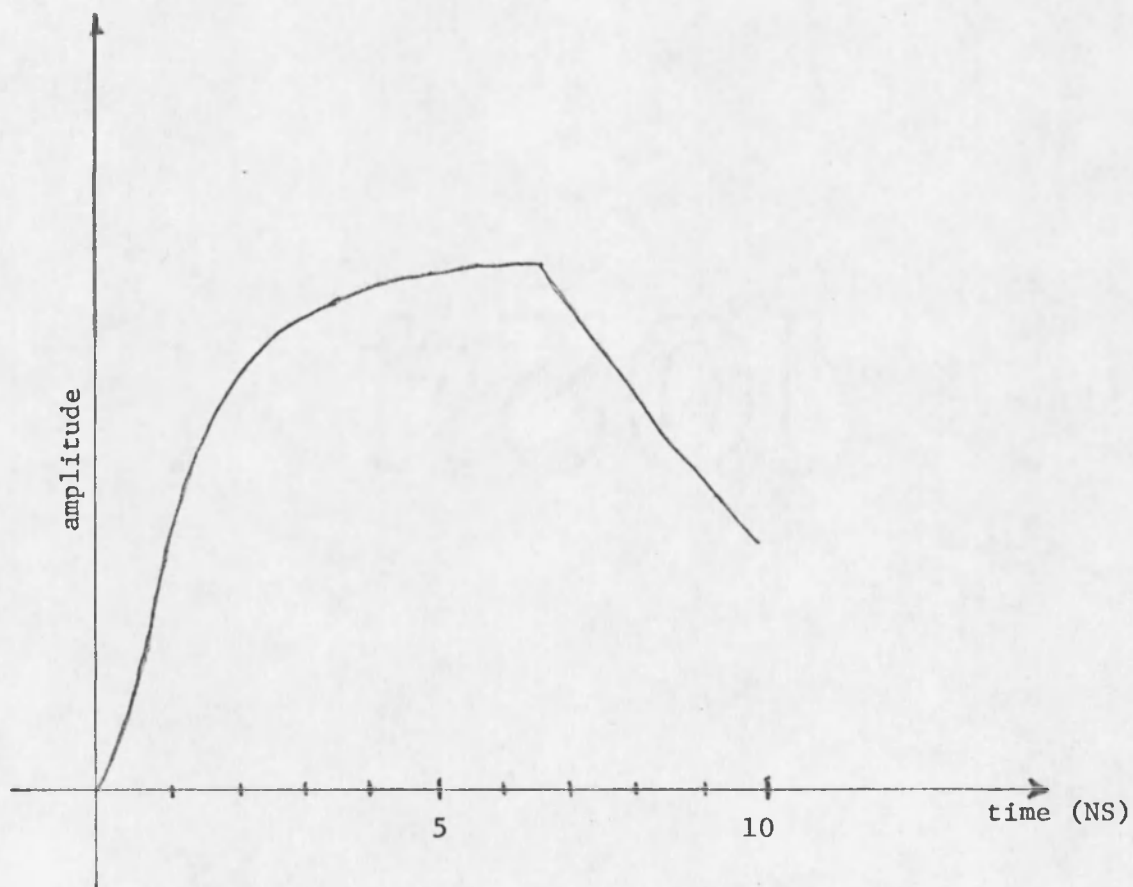


Fig. 2.20 Refined Reflected Signal from Model Tower

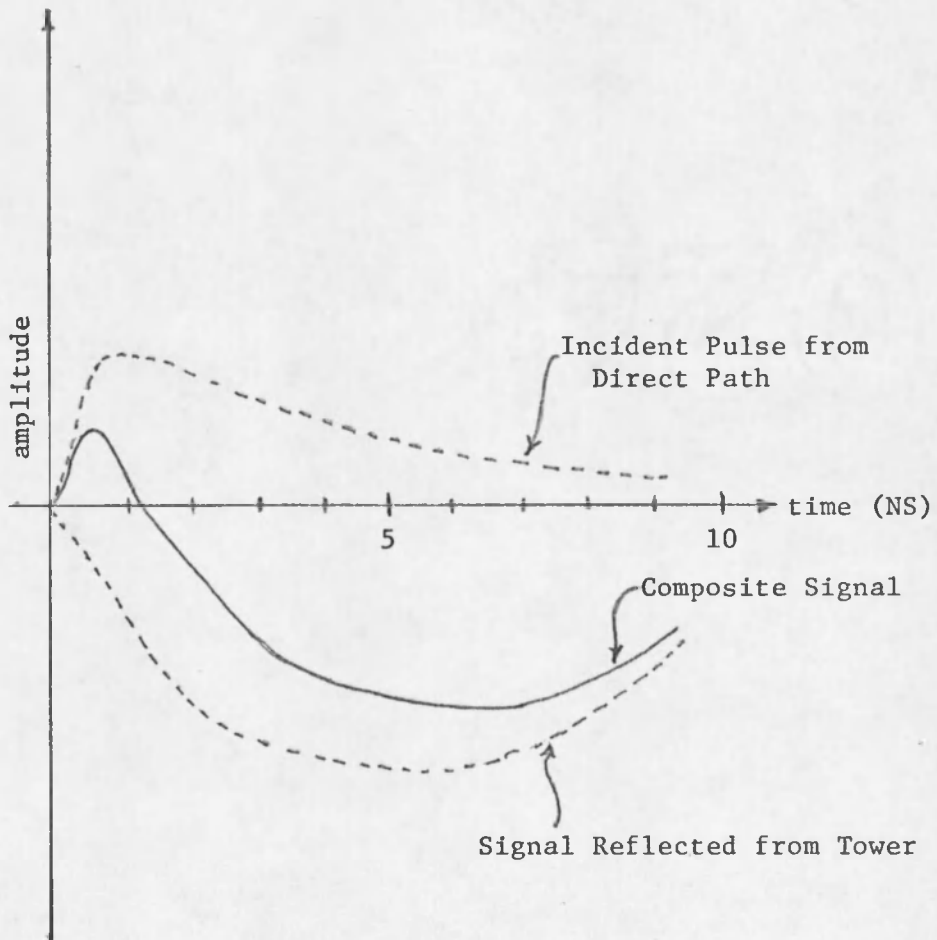


Fig. 2.21 Refined Estimated Sensor Response

To determine how the amplitude of the incident wave varied with distance, an H-field sensor was mounted in the center of a large metal plate and measurements were taken at various distances from the source monopole. Using the physical optics approximation that the measurements are proportional to twice the amplitude of the incident H-field, the relationship between the incident wave and the distance from the source can be determined. The results of the test are shown in Fig. 2.22 which is a plot of normalized amplitudes versus $1/R$. A line representing an idealized $1/R$ dependence is also shown. For the region occupied by the model communications center, .09 to .125 on the horizontal axis, the incident wave exhibits very good $1/R$ dependence.

To determine if the output of the pulse generator was being distorted by something in the EMP source system, a comparison was made between shape of the pulse just after it leaves the pulse generator and again after it was radiated from the source monopole and received by an H-field sensor. It was realized at the time of this test that if distortion was present, the test would be inconclusive because the distortion could have been caused by something in the measurement system. However, if there was no distortion, the test would serve a dual purpose in that the capability of the H-field sensor to reproduce the incident waveshape would also be verified.

The H-field sensor was installed in the center of a square sheet of aluminum which would provide 2 NS of clear time before edge reflections would interfere with the sensor response to the incident wave. The pulse generator was set up to produce a pulse with a 1.2 NS pulse

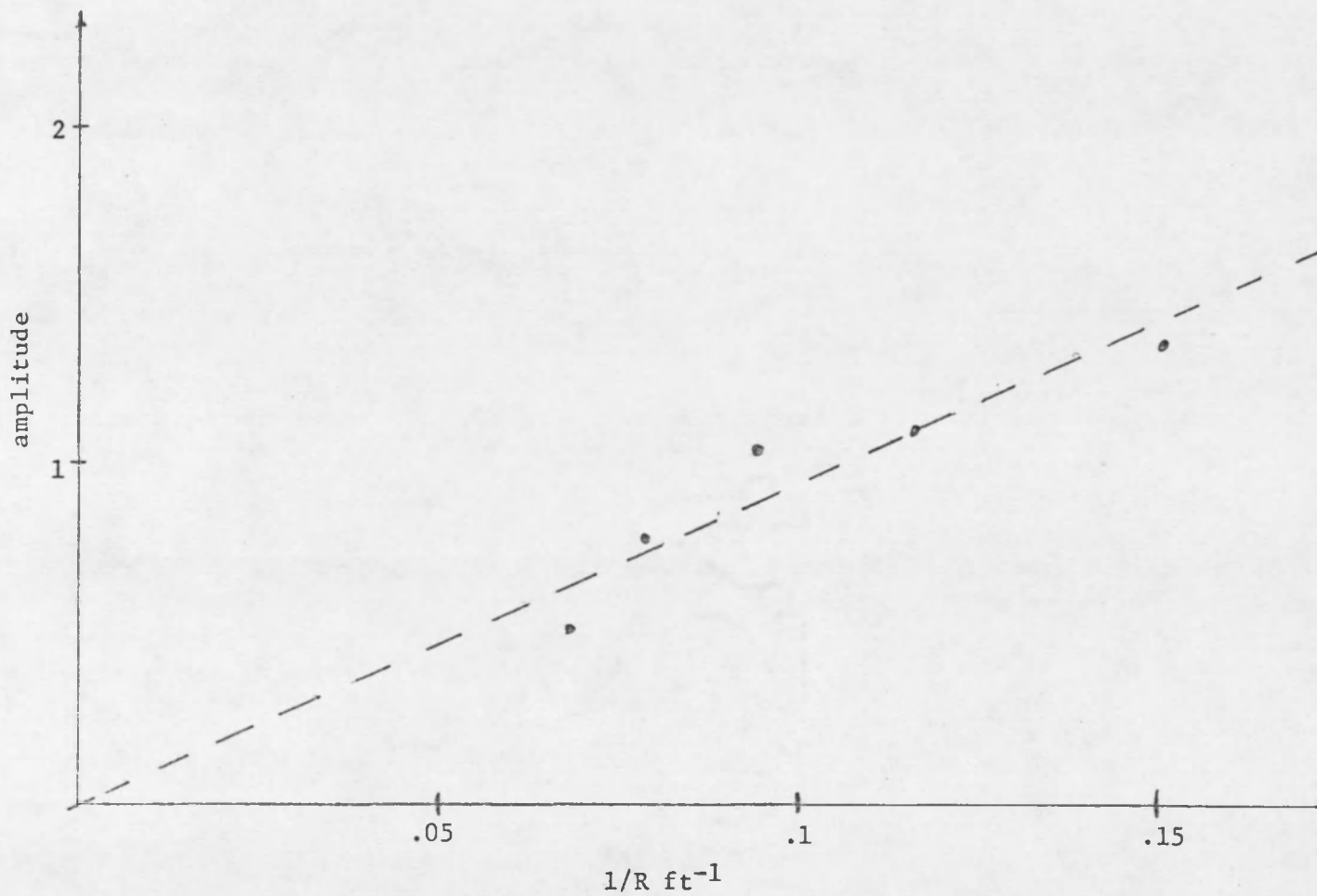


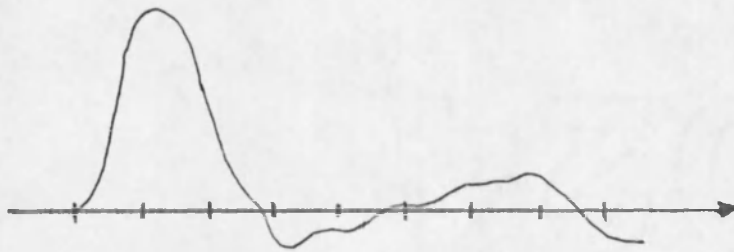
Fig. 2.22 Incident Pulse Peak Amplitude (Normalized) as a Function of 1/R

width at the 50% points and the output was recorded. The pulse was then radiated from the source monopole and received by the H-field sensor mentioned above at a distance of 2.745 mtrs. from the source monopole. The amplitude of the pulse was adjusted to the same value as that recorded from the pulse generator and the pulse shape was recorded. The results, as shown in Fig. 2.23, were that there was exact agreement between the two pulse shapes for the first 2 NS thus proving that the source and measurement systems did not distort the pulse output of the pulse generator.

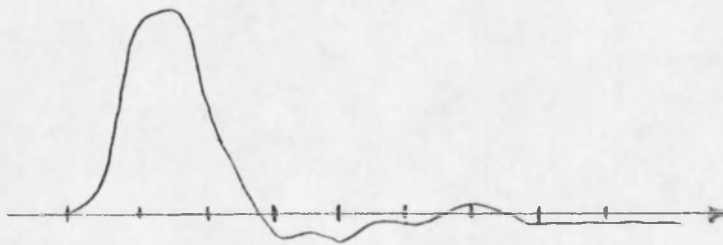
Data Repeatability Test

During the data taking phase of this project, the model configuration had to be changed many times in order to make the desired measurements. These changes included such things as rotation of the sensor units, rotation of the tower with respect to the building, disconnecting and reconnecting the guy wires and rotation of the entire model area. To insure that the model could be reconfigured once the configuration was changed, two sets of data were taken with a time interval between them of twelve days. During this interval, the model configuration was changed several times to facilitate other measurements. Also, since the data to be compared were from different model configurations, the test would show how well different configurations could be reproduced.

The results of the test can be seen in Figures 2.24 and 2.25. There are some slight differences between the two sets of data; however, this can be explained by the presence of background noise.



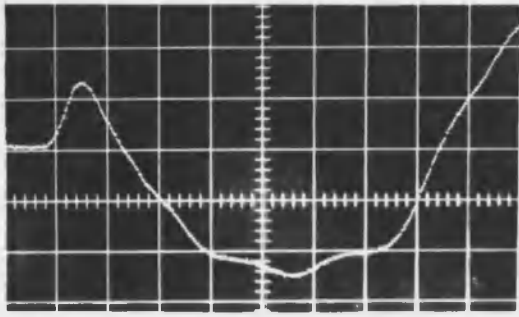
(a) Radiated Pulse



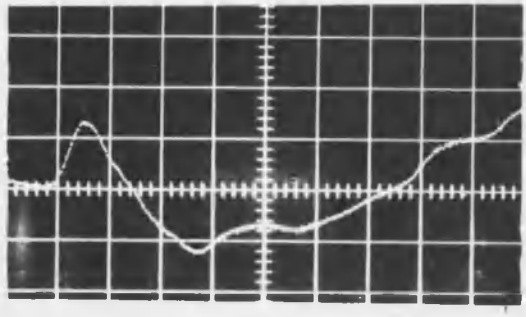
(b) Pulse Generator Output

Horizontal Scale - 1 NS/Div.

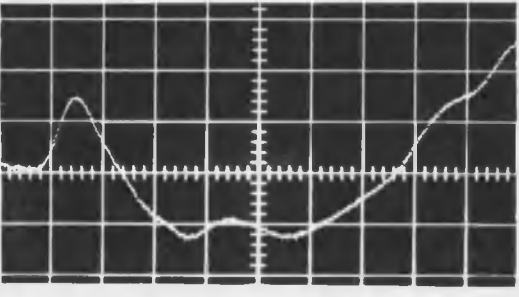
Fig. 2.23 Comparison of Pulse Generator Output with Radiated Pulse



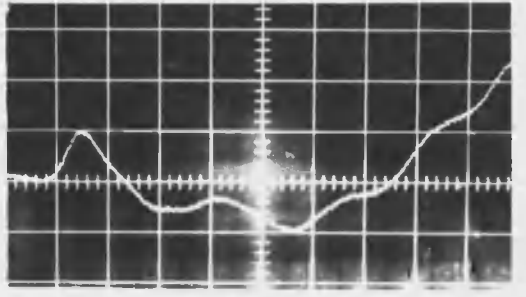
a



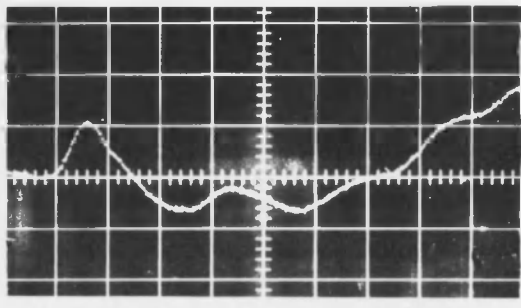
b



c

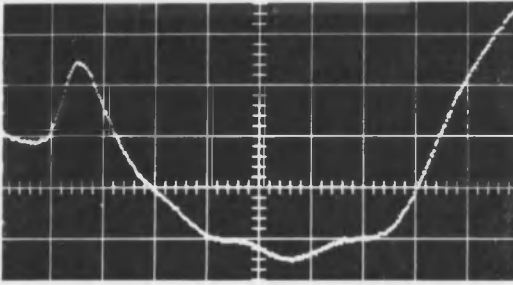


d

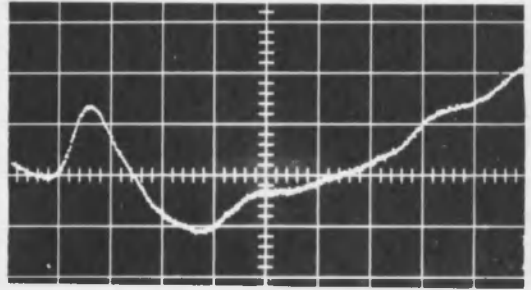


e

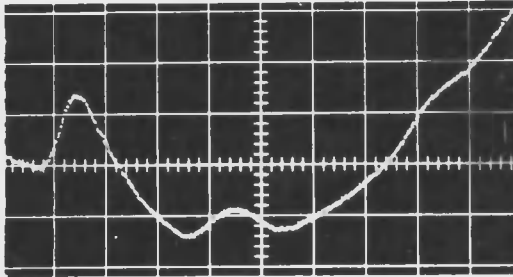
Fig. 2.24 Repeatability Test Data #1



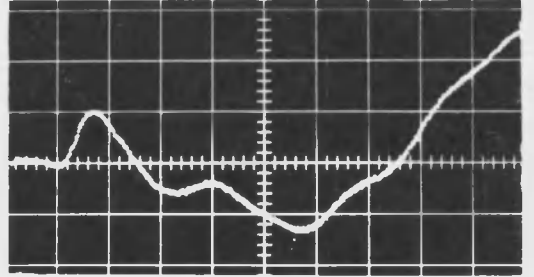
a



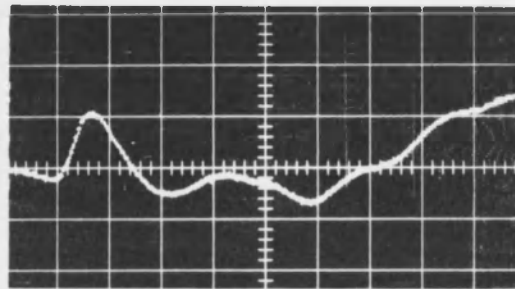
b



c



d



e

Fig. 2.25 Repeatability Test Data #2

Performance Evaluation

The overall performance of this simulator was judged to be very good in that it produced all of the required conditions for the study. The only negative feature of the simulator was the lack of versatility available from the EMP source. It would have been more desirable to be able to produce a TEM wave of either polarity with a variable angle of incidence.

CHAPTER 3

FABRICATION AND TESTING OF A 1/20 SCALE MODEL

PARALLEL PLATE EMP SIMULATOR

Construction of Test Facility

Ground Plane

The ground plane used for this study was essentially the same one as described previously. The surface of the ground plane was cleared of non-essential structures to prevent unwanted reflections from interfering with the measurements to be made. A .915 x 1.525 mtr. piece of sheet metal was placed on the surface of the ground plane to serve as a reflecting surface for signals contained within the parallel plate structure. It would also provide a means for mounting field sensors in the region between the plates at their intersection with the ground plane. Further, it would provide a smooth surface which would insure that the plates were in contact with the ground plane in the region of the intersection between the plates and the ground plane.

Parallel Plate Structure

The plates of the structure were made by stretching aluminum screen over a wood frame to form a continuous parallel plate guide from the source to the load (Fig. 3.1). The edges of the screen were stapled to the frame along the top and bottom of the plates. In some places, it was necessary to splice sections of the screen material together in order

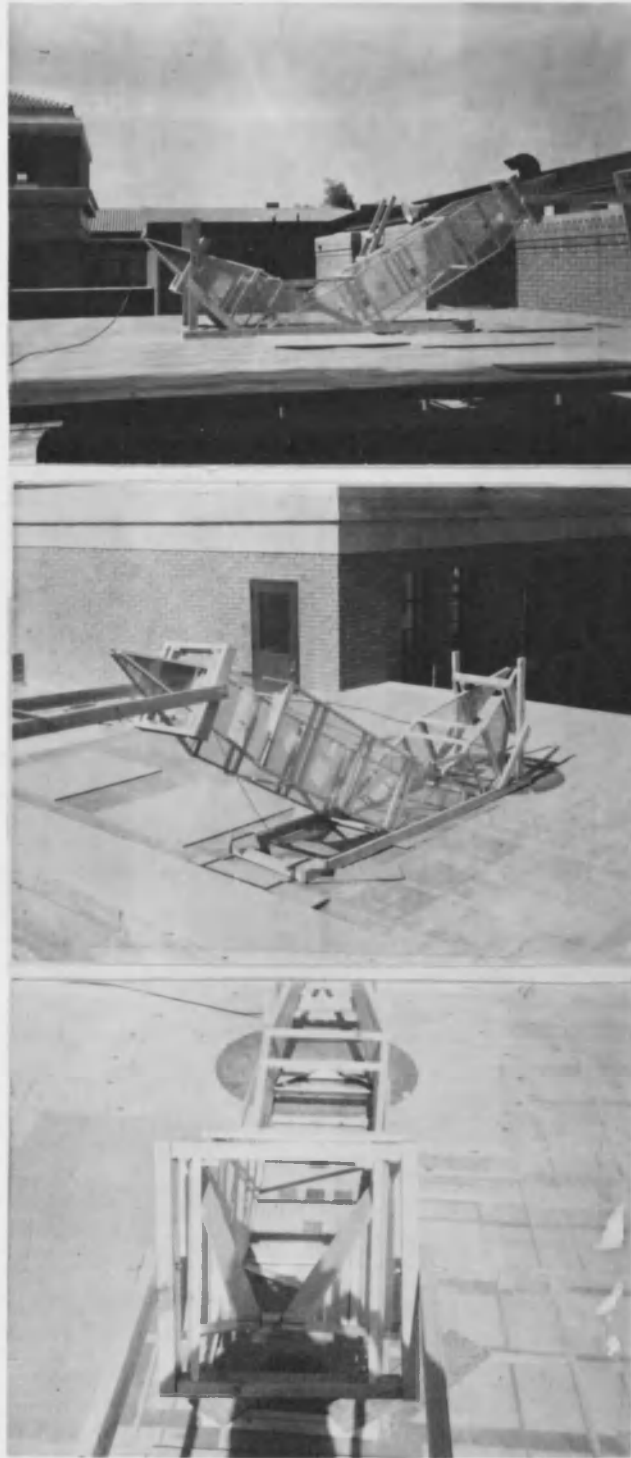


Fig. 3.1 Model EMP Simulator

to follow the contour of the plate structure. Where possible, the ends of the splices were overlapped and stapled to part of the wood frame. Where this was not possible, the ends were overlapped and woven together with strands of the aluminum screen material. In the region where the plates were to intersect the ground plane, the screen material was folded over the bottom of the framework and stapled. This would insure that the plates were in contact with the ground plane.

The plates are vertically oriented and intersect the ground plane at an angle of 30° with respect to horizontal. The cross-sectional dimension of the structure is .61 mtrs. square. Plate separation is maintained by braces across the top and bottom of the plates. Vertical support for the structure is provided through the braces and mounting structures of the source and load TEM horns which are attached to opposite ends of the parallel plate structure. Figure 3.2 gives the overall dimensions of the structure including the source and load TEM horns.

The load section of the structure is designed to absorb energy which is reflected from the ground plane in the region between the plates at their intersection with the ground plane. A TEM horn was used as a transition stage between the .61 mtrs. square cross-sectional dimension of the plate structure and the load. A full description of the horn construction will be given in the section concerning the EMP source since the load and source horns are identical. The load attached to the horn consists of a 12.2 mtr. length of shielded twin lead which has approximately the same characteristic impedance as the horn. The length of the

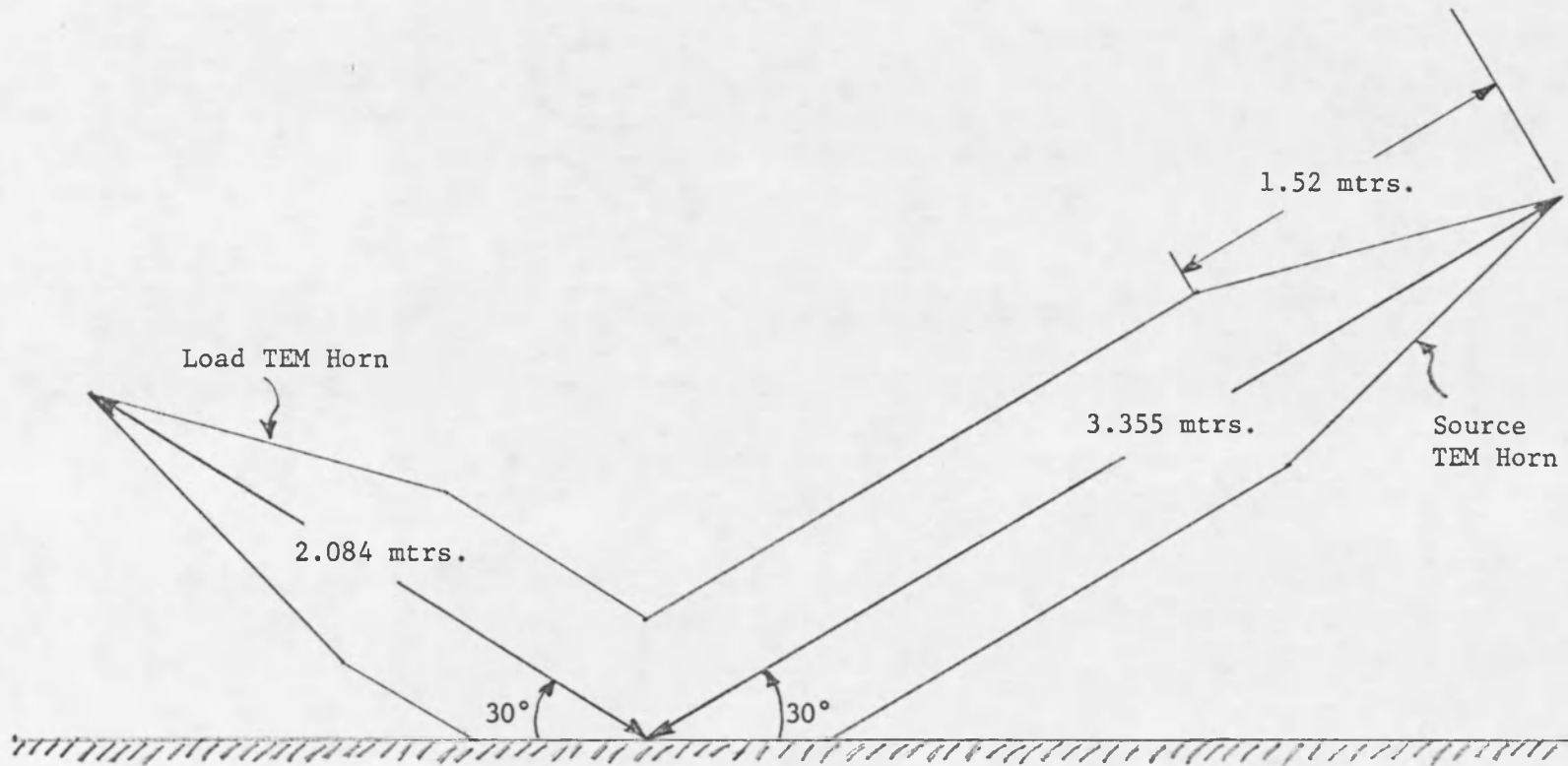


Fig. 3.2 Model Dimensions

twin lead load would insure that signals reflected from its end would be delayed a sufficient amount of time so that they would not interfere with any measurements to be made. The twin lead to TEM horn connection was matched using a time domain reflectometer. The results of tests performed to determine how good a match this connection was will be discussed later in the EMP source tests section of this study.

Part of the framework for the plate structure was designed to facilitate the mounting of field sensors for the measurement system. The connection for the sensor signal cable had to pass through the screen material which meant that there would be a hole in the screen at each sensor location. These holes were sufficiently large enough to perturb the fields if left exposed. With a sensor installed, the hole would be covered by the sensor mounting plate. However, to minimize perturbations caused by the sensors, only one sensor at a time would be in place. Thus, blank plates of the same dimensions as the sensor mounting plates were installed at each sensor location when it was not in use. The same precautions were used for sensor locations on the reflecting plate in the region between the parallel plates at their intersection with the ground plane.

EMP Source

The EMP source consists of a high voltage DC power supply, a pulse generator, a TEM horn and interconnecting cables. Figure 3.3 is a block diagram of the EMP source.

The DC power supply is a Polytechnic type 812 klystron power supply. The beam voltage output of this unit is used for the generation of

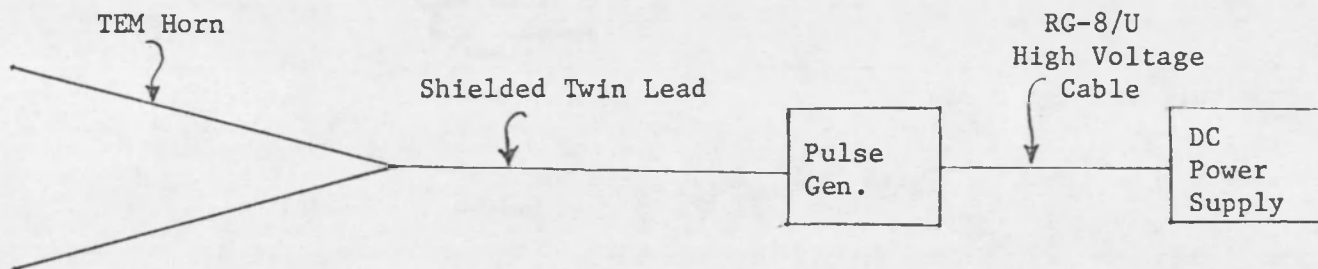


Fig. 3.3 EMP Source Block Diagram

the high voltage pulse. It is connected to the pulse generator through a section of RG-8/U coaxial cable.

The pulse generator unit, designed and built at The University of Arizona, is self-contained except for the high voltage DC power supply used for the pulse output. It has the capability of producing several pulse shapes of variable duration and repetition rate. For this study, the unit produces a double exponential type pulse with a rise time of approximately 550 PS and a fall time ($1/e$) of approximately 6.5 NS. The pulse is generated by discharging a capacitor through a mercury-wetted reed switch (Fig. 3.4) into a load resistance. The switch and capacitor were built into a section of shielded twin lead with the capacitor connected across the two conductors of the twin lead as close as possible to the switch. A current limiting resistor is connected to the twin lead conductor containing the switch and the other conductor and shield are grounded. The switch is energized by a coil wound around the twin lead cable in the vicinity of the switch. The pulse generator was constructed in this manner to eliminate the necessity of using some type of adapter between the pulse generator and the twin lead signal cable which could cause unwanted reflections and pulse distortions. Pulse amplitudes of 300 and 1000 volts and a repetition rate of 200 PPS were used for this study.

The TEM horn is used primarily as a transition stage between the twin lead geometry and the .61 mtr. square cross-sectional dimensions of the parallel plate structure. It consists of two 1.22 mtr. long tapered plates (Fig. 3.5). Half of each plate is solid brass and the other half

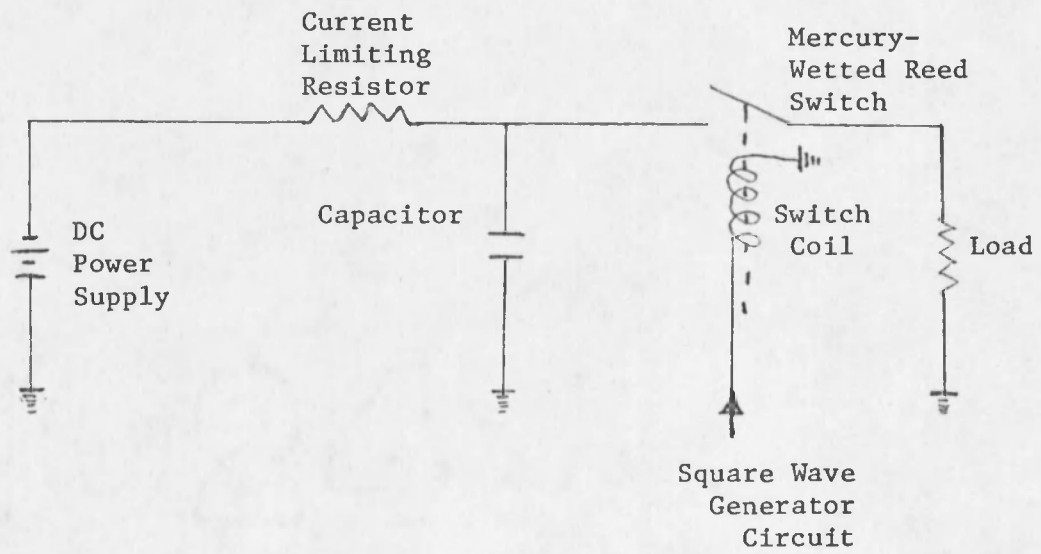
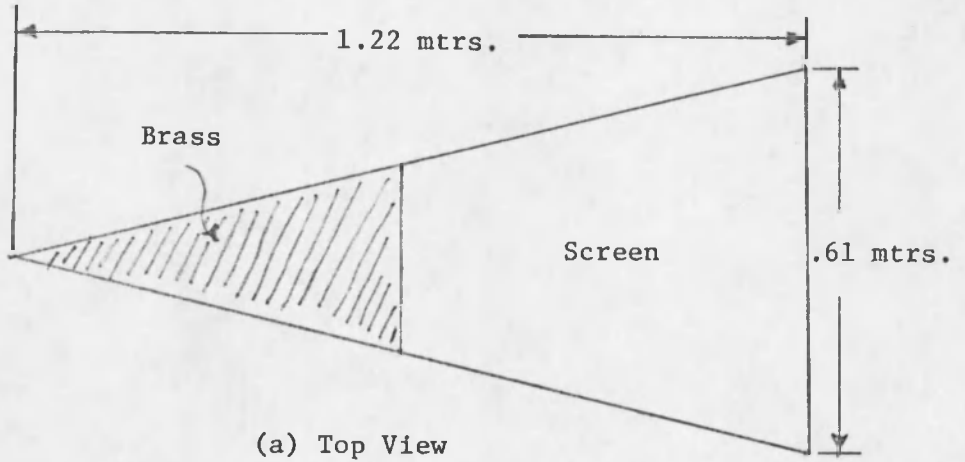
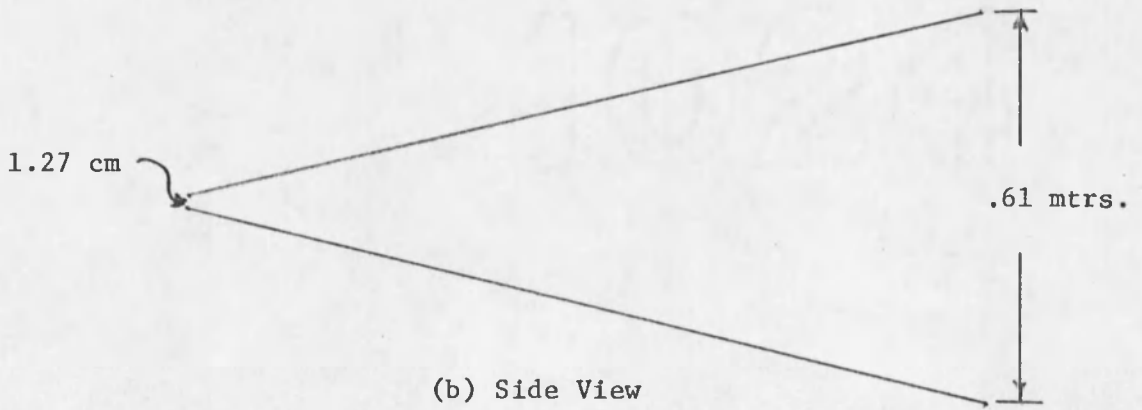


Fig. 3.4 Pulse Generating Circuit



(a) Top View



(b) Side View

Fig. 3.5 TEM Horn

is aluminum screen. This material is mounted to a wooden frame for rigid support. The screen material actually extends 5.08 cm. beyond the horn so that it can be stapled to the parallel plate structure to form a continuous conducting surface.

The plates of the horn are mounted inside a wooden framework in such a manner that they can be freely positioned and locked in place. This framework also serves as the mounting points of the supporting structure for the horns. The entire structure was designed with the idea in mind that it might be used independent of the parallel plate structure at some later date. The horn could serve as a radiating element which would be highly versatile in that it could produce a TEM wave of either horizontal or vertical polarization for all angles of incidence. The load TEM horn was constructed in the same manner as described for the source horn. The connection between the source horn and the twin lead signal cable from the pulse generator was matched using a time domain reflectometer. The quality of this match will be discussed later in the EMP source tests portion of this study.

The signal cable between the source horn and the pulse generator is a 3.05 mtr. length of shielded twin lead. The length was chosen to provide approximately 20 NS of delay before a reflection signal from the twin lead to horn connection could interfere with any measurements being made.

Measurement System

The measurement system consists of a Tektronics type 567 readout oscilloscope, with type 6R1A digital unit, type 3T77 sampling sweep and

type 3S76 sampling dual trace plug-in units, a polaroid CR-9 oscilloscope camera, E-field probes, a Burr-Brown model 6000 analog computer and a Hewlett-Packard model 7035A, x-y recorder.

The oscilloscope with the plug-in units indicated, has a rise time capability of 400 PS and an input impedance of 50 ohms, a peak-to-peak normal noise level of 2 MV. The oscilloscope uses a sampling process to produce high resolution without jitter. It also has external outputs that provide analog signals from the CRT presentation.

The camera used has the capability of manually timing the exposure which, when used with the single display feature of the oscilloscope, produces a good resolution picture of the CRT display.

The E-field probes are short (12 cm) monopoles mounted on a 10.16 cm. square plate in the same manner as shown in Fig. 2.15. The response of the probe to an incident wave is proportional to the time derivative of the incident E-field [Schmitt, Harrison, and Williams, 1966]. For the length of probe being used, there will also be some oscillations present, the period of which will correspond to the resonant wavelength of the probe; approximately 1.6 NS. This same type of probe was used as a reference monitor and trigger for the oscilloscope. This was done to insure that the same signal was being generated throughout the test phase. Figure 3.6 shows the location and number of the test points where these probes were used. Since E-field measurements were the primary concern of this study, no other types of probes were used.

As stated earlier, the output from the E-field probe is proportional to the time derivative of the incident E-field. To analyze the

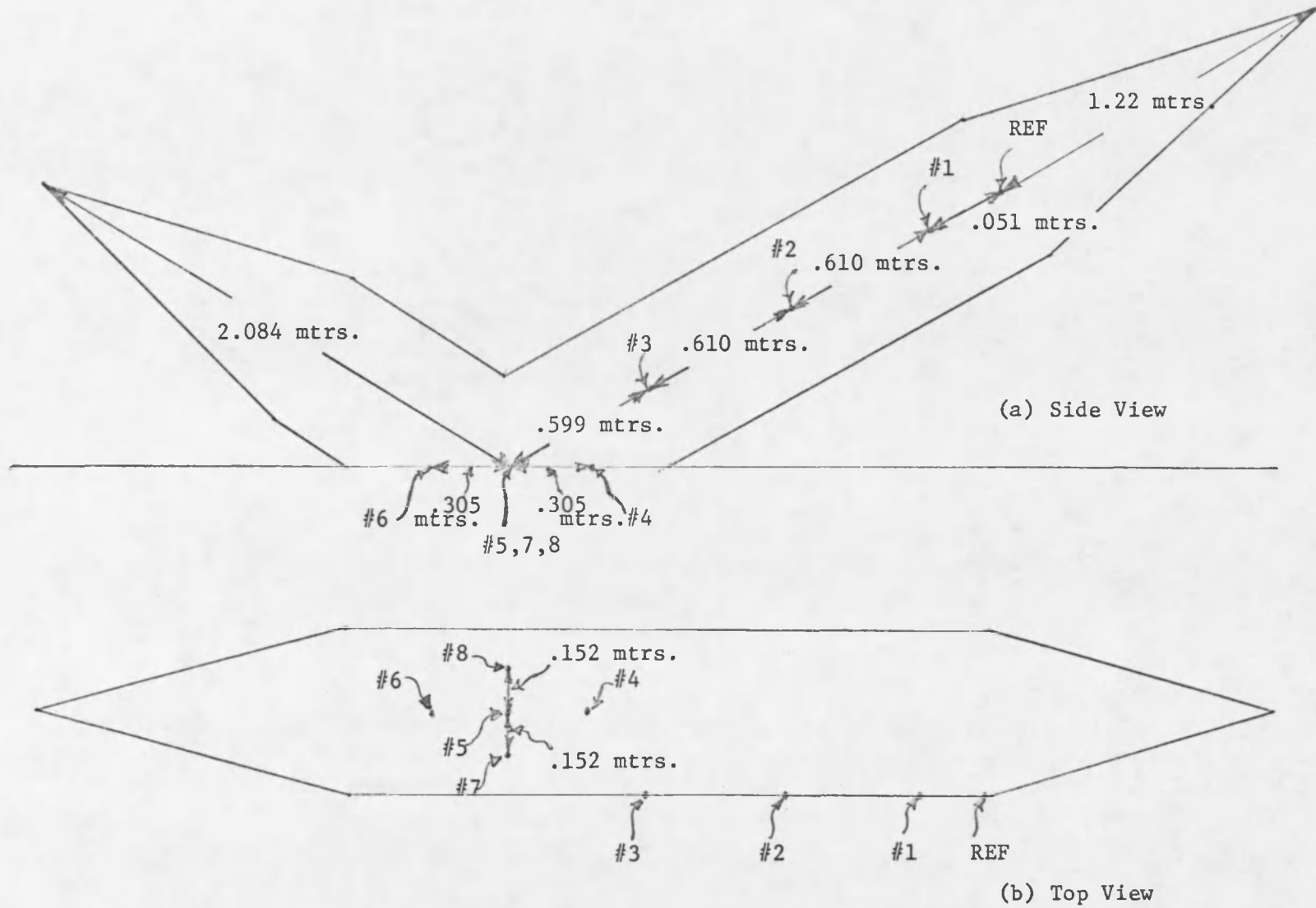


Fig. 3.6 Test Point Locations

data taken, it was necessary to develop a method which would integrate the E-field probe response and provide a permanent record of the results. To do this, the analog output from the vertical channel on the oscilloscope was fed to the Burr-Brown analog computer where it was integrated. The integrated signal was then sent to the vertical input of the x-y recorder. The horizontal input to the recorder was provided by the sweep output terminal on the oscilloscope. Figure 3.7 shows a block diagram of this arrangement. The entire setup was tested to insure that the recorded data was valid. The methods used for the test and test results will be presented in the measurement system tests portion of this study.

The signal cable used for the reference monitor and trigger pulse E-field probe was a 9.15 mtr. length of RG-58A/U. While this amount of this type of cable might cause distortion of the sensor output, it was not critical in this application because it would not be used for data taking purposes. The signal cable used in conjunction with the measurement E-field probe was a 9.15 mtr. length of RG-214/U. This type of cable is of much better quality than RG-58A/U and distortion caused by it should be at a minimum.

Tests

Measurement System Tests

Tests performed on the measurement system were used to determine such things as noise level and the validity of the integrated E-field probe response.

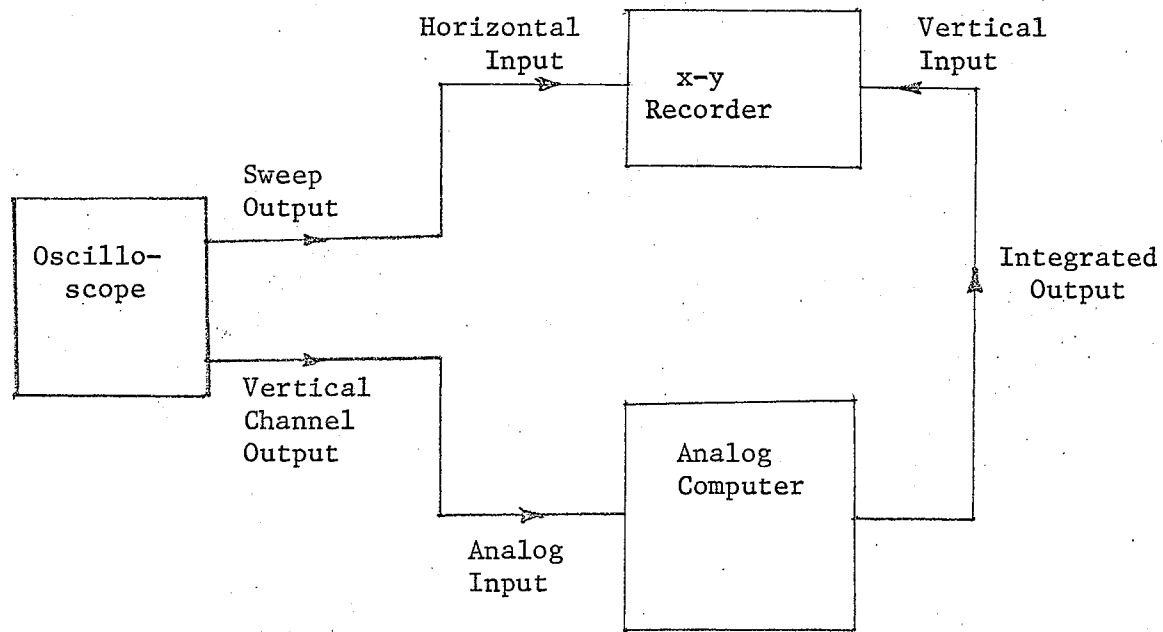


Fig. 3.7 Block Diagram of Integrating and Recording Setup

The need to use equipment other than the oscilloscope for the purpose of taking data made it necessary to find a location which would sufficiently shield this equipment from external noise. Thus, the oscilloscope, analog computer and x-y recorder were placed in a room beneath the ground plane. The room is isolated from the outside by a double ceiling which contained a wire mesh. The signal cables were routed through an air vent to the simulator on the roof. Noise interference tests were performed both with and without the external equipment connected to the oscilloscope. There was no noticeable difference in the oscilloscope presentation for the different configurations which indicates that the external connections were not introducing noise into the system. Another indication of the amount of noise being introduced into the system is to note the level of signal present on the data presentation just prior to the arrival of the incident pulse. In all cases, there was virtually no signal present prior to the arrival of the incident pulse, which can be seen in Fig. 3.13 as an example.

As mentioned before, to analyze the output from the E-field probe, it was necessary to develop a method which would integrate the probe output. The most convenient way available was to integrate the analog output of the vertical unit on the oscilloscope. Since the Burr-Brown analog computer has a ready-made integrating capability, it was decided to use this unit instead of designing a separate integrating circuit. The major problem encountered with this unit was that it integrated on a 10 second time base. What this means is that if the analog signal to be integrated has a duration of only five seconds, the resultant integration

will have an amplitude value which is exactly half of the actual value. This fact is important because the time base for the analog signals from the oscilloscope is determined by the sampling rate of the oscilloscope and the pulse repetition rate of the pulse generator. Thus, the time base may not be 10 seconds and the integrated signal will not have the correct amplitude. To test this hypothesis, a square wave pulse (Fig. 3.8) was fed into the oscilloscope at the rate of 200 PPS which resulted in a five second horizontal sweep time. The pulse is two units wide and three units tall and thus should have an amplitude of six units when integrated. As can be seen in Fig. 3.9, the amplitude of the integrated signal is only three units which is exactly half the correct value. With this hypothesis established, the error can be corrected by simply adjusting the gain of the integrator according to what the time base is for the analog signal.

A second test of the integrator was performed using the same type of signal as would be expected from the simulator. To do this, a double exponential type of pulse was fed into a transmission line above a ground plane. The electromagnetic wave was detected by a short monopole mounted on the ground plane beneath the transmission line and its response was recorded (Fig. 3.10). This response was then integrated using the Burr-Brown analog computer with a compensating gain factor in the integrating circuit. The result is shown in Fig. 3.11. To verify that this represents the true integrated value of the input signal, the input signal was graphically integrated and plotted (Fig. 3.12). A comparison of Figures 3.11 and 3.12 shows that the two plots are almost identical thus verifying the operation of the integrator.

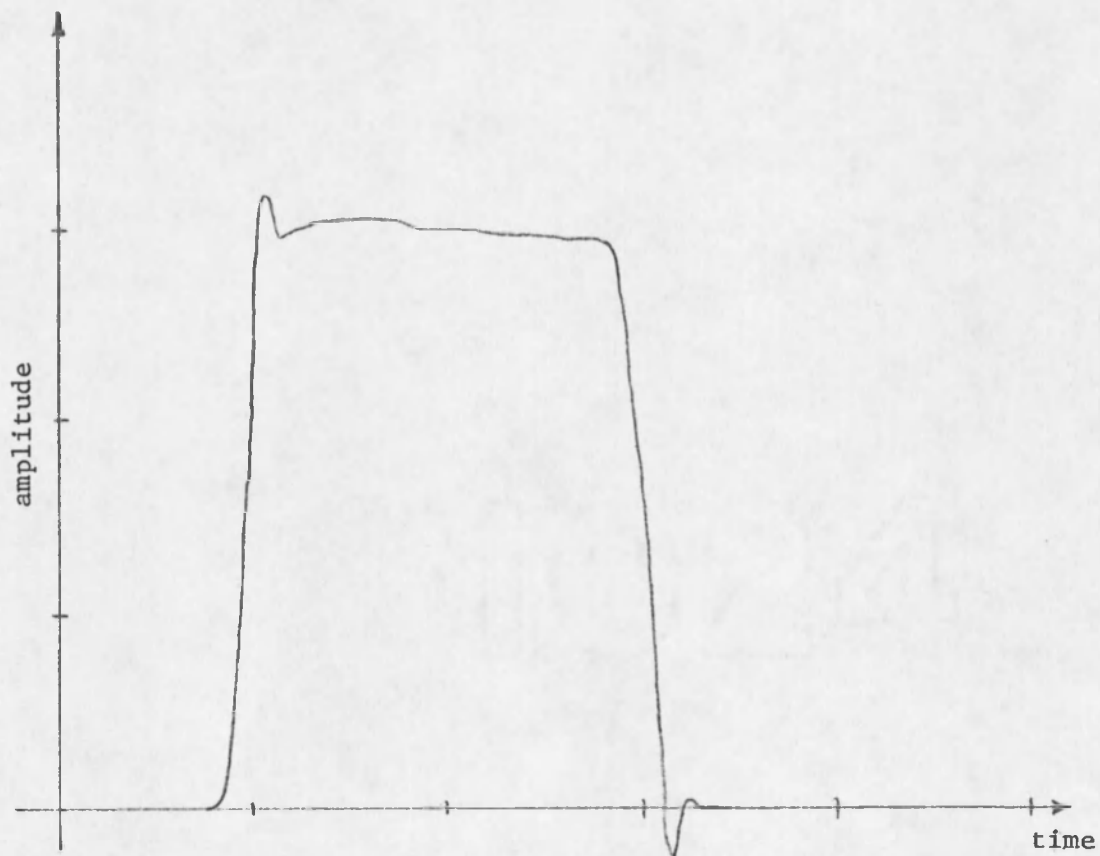


Fig. 3.8 Square Wave Input to Integrator

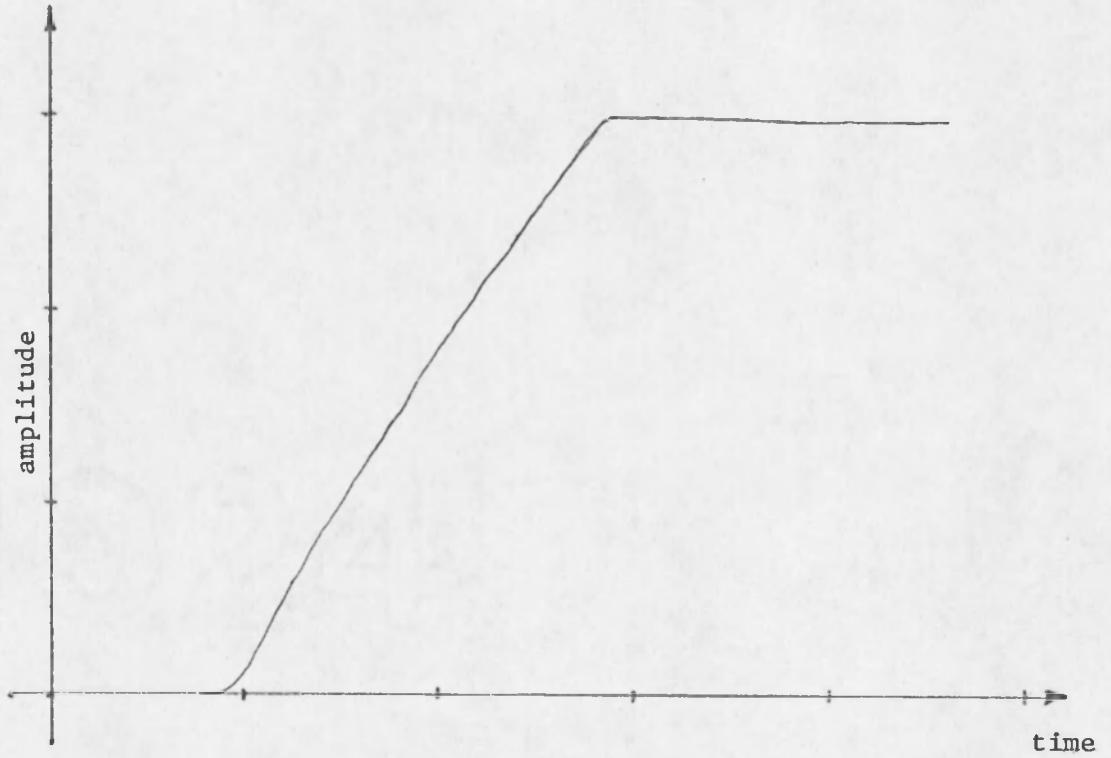


Fig. 3.9 Integrator Output with Square Wave Input

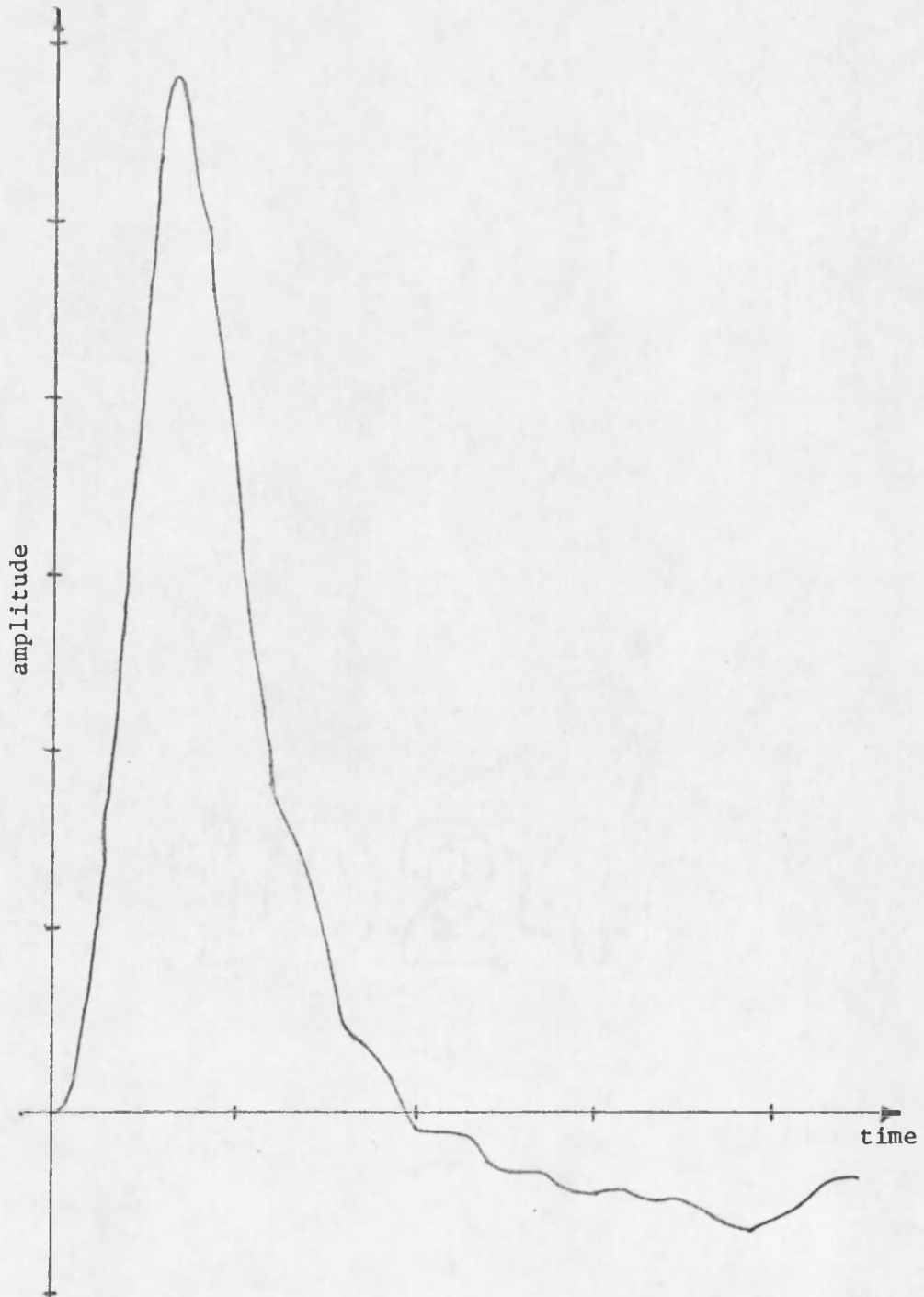


Fig. 3.10 Short Monopole Response to Double Exponential Pulse Input

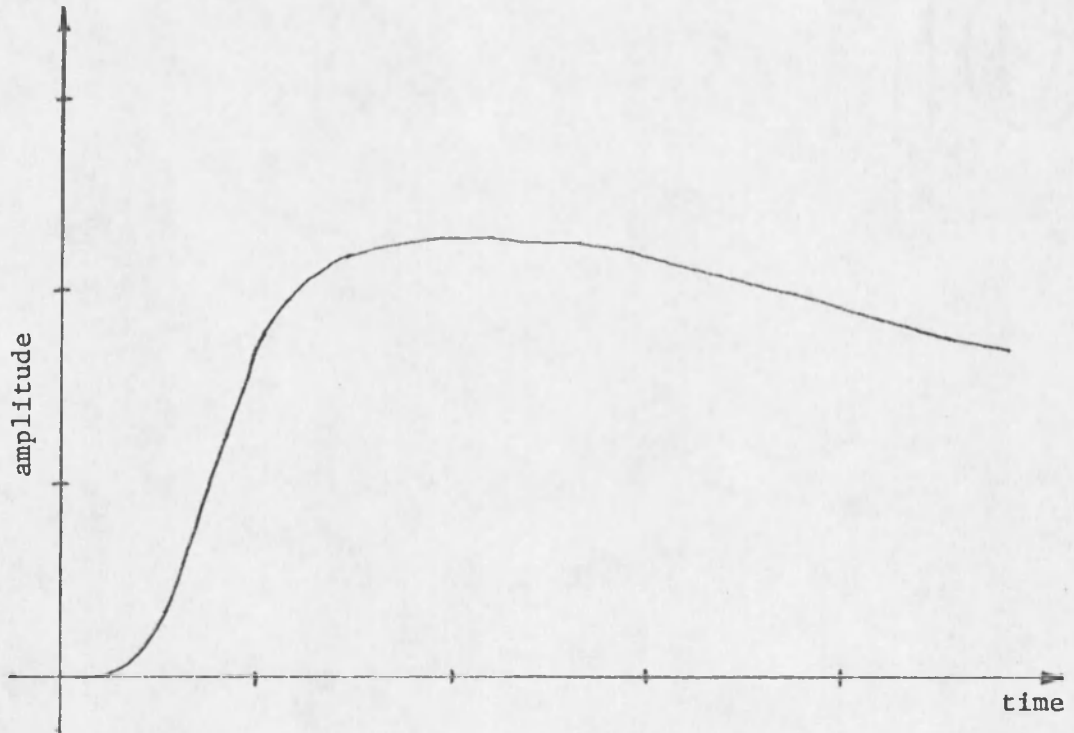


Fig. 3.11 Integrated Short Monopole Response to Double Exponential Pulse Input

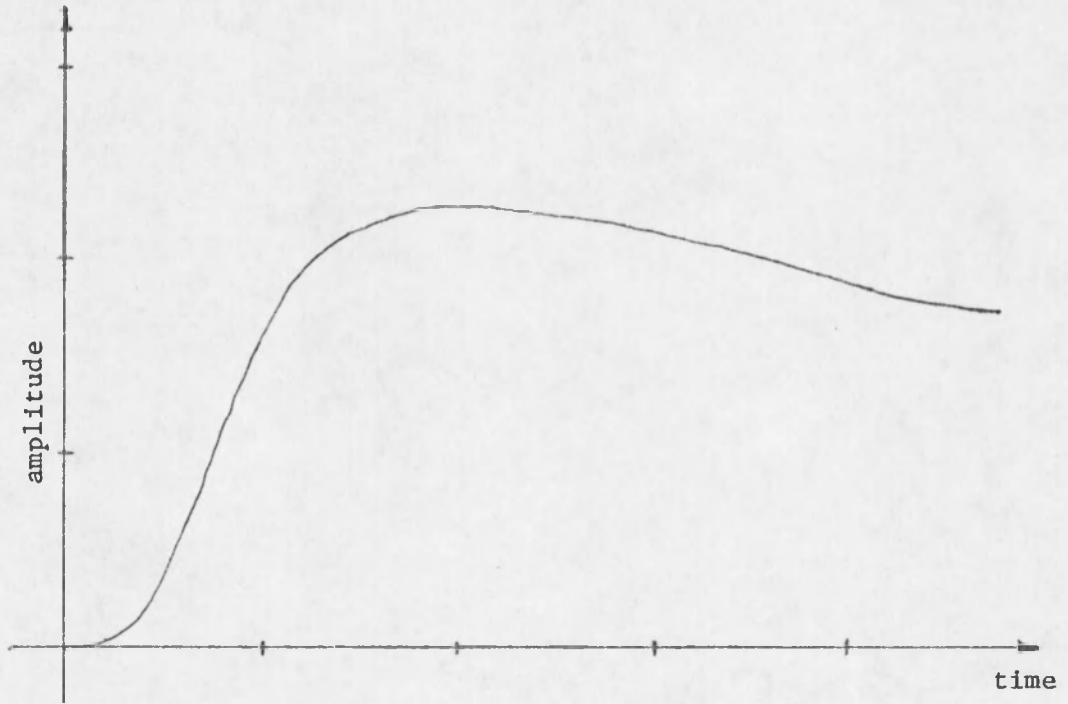
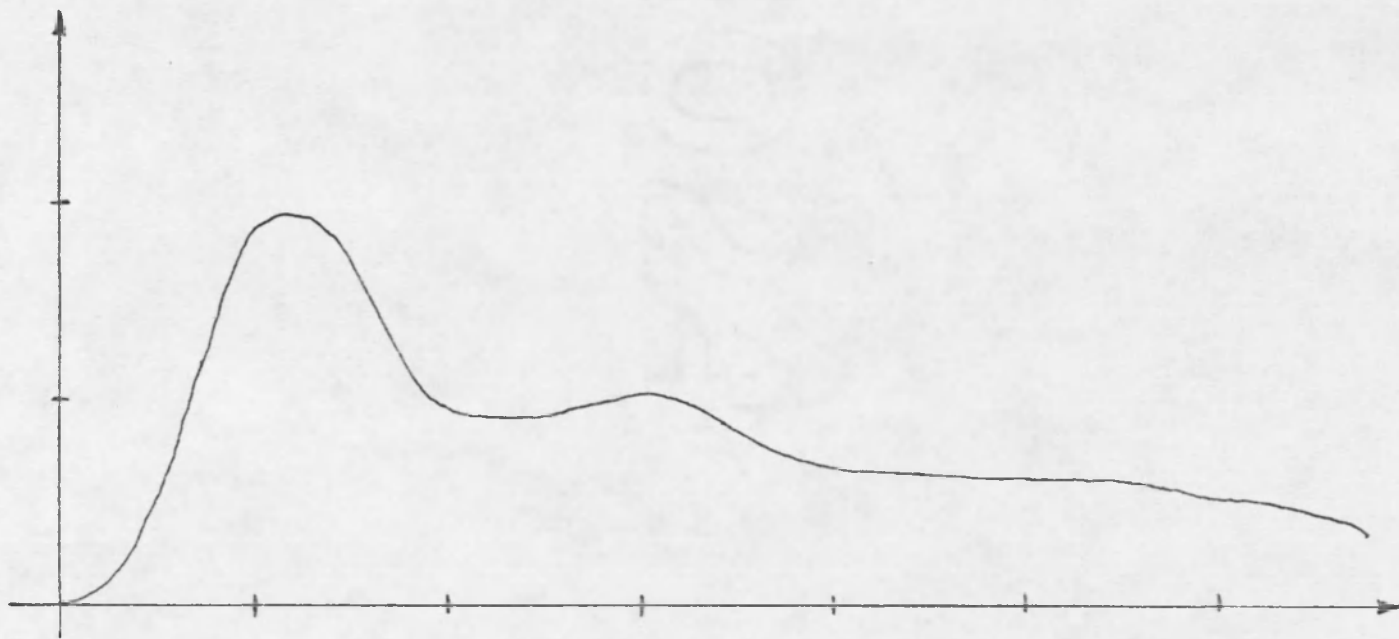


Fig. 3.12 Graphically Integrated Short Monopole Response to Double Exponential Pulse Input

EMP Source Tests

The EMP source was tested to determine the fidelity of the source output as compared to the pulse input and the quality of the connection between the source TEM horn and the twin lead signal cable from the pulse generator.

Because of the length of the E-field probe used in the measurement system, it was expected that there would be oscillations present in its response to the incident wave which would not be present in the wave front itself. Reducing the length of the probe in an attempt to remove these oscillations resulted in a reduction in amplitude of the probe response to the point where it became comparable to the noise present in the system. It was decided, however, that enough information about the source output could be gained from the longer probes. Of primary interest in this test was the determination of whether or not the pulse rise time was being degraded and if the pulse shape was being drastically distorted. To reduce the possibility of reflections from some point in the simulator interfering with the data taken for this test, it was decided to observe the source output as close as possible to the source TEM horn. Thus, the reference probe output was selected to be analyzed. The RG-214/U signal cable was attached to this probe and its output was integrated and recorded. The results can be seen in Fig. 3.13. The rise time of this pulse is slightly less than 600 PS, which is in good agreement with the pulse output from the pulse generator, and the pulse shape is essentially that of a double exponential. The oscillations due to the length of the monopole can best be seen in Fig. 3.14. As can be seen, the period of



Horizontal = 1 NS/Div

Fig. 3.13 Integrated Response from Reference E-Field Probe

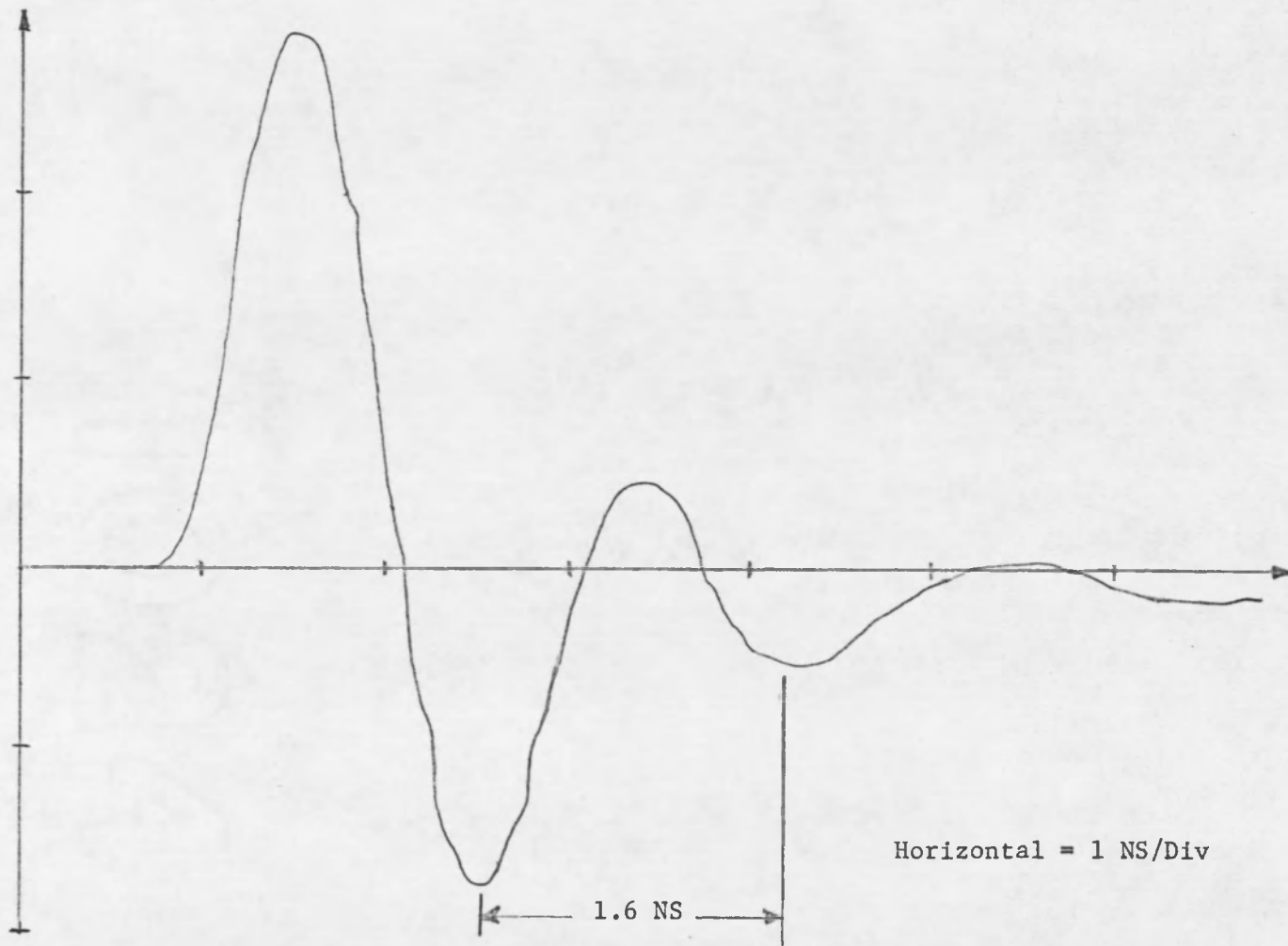


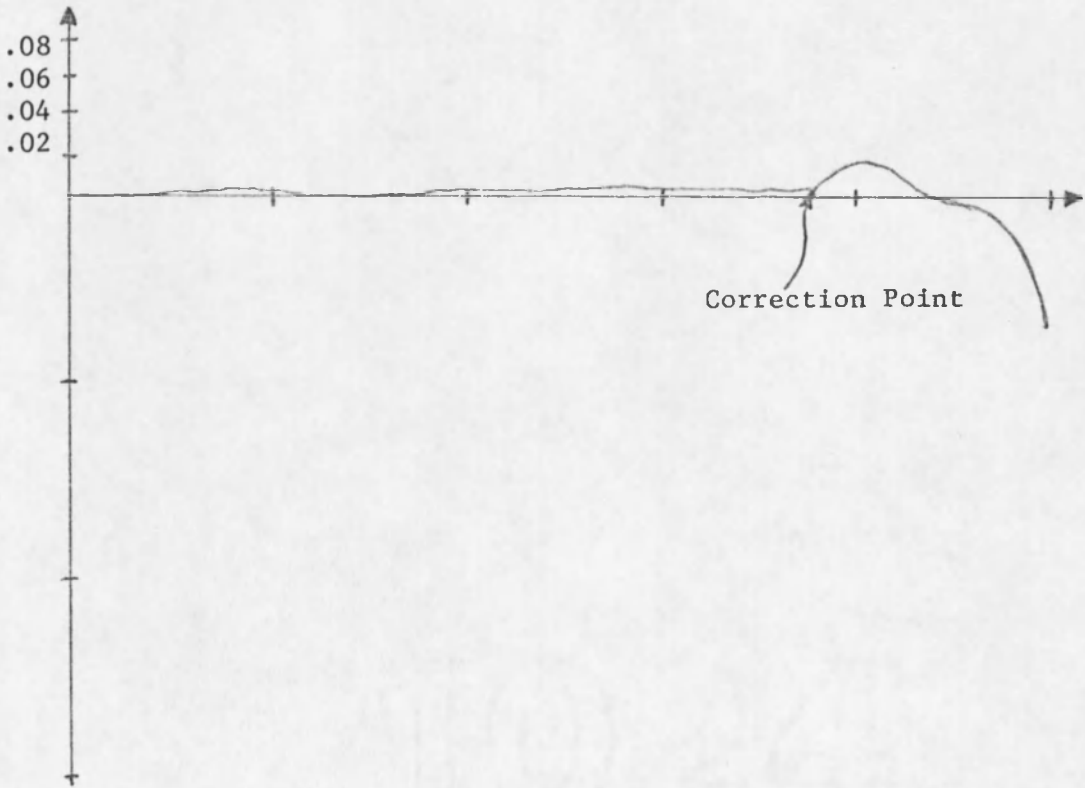
Fig. 3.14 Non-Integrated Response from Reference E-Field Probe

the oscillation is approximately 1.6 NS which corresponds to a quarter wavelength of 12 cm and agrees very well with the stated length of the monopole.

To transfer the maximum amount of energy from the pulse generator to the parallel plate structure, the connection between the source TEM horn and the shielded twin lead cable from the pulse generator has to be as close to a perfect match as possible. A measurement that can be made to determine the quality of a connection of this sort is the magnitude of the reflection coefficient at the connection point. To make this measurement, a time domain reflectometer (TDR) was used. The magnitude of the reflection coefficient for the connection was less than .02 which means that the connection was very good. Figure 3.15 is a representation of the TDR measurement. The connection between the load TEM horn and the twin lead cable used for the load was tested in the same manner and found to be as good as that just described. This means that almost all of the energy entering the load horn is being transferred to the load and very little is being reflected back into the parallel plate structure.

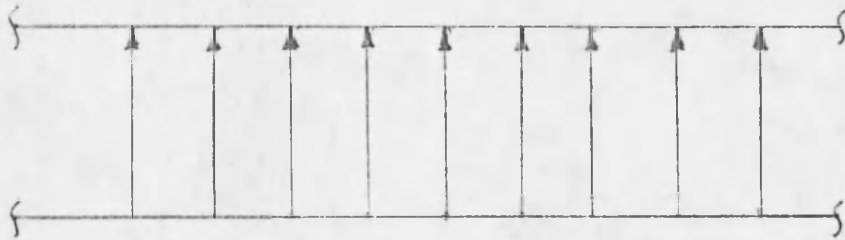
Cross-Polarized E-Field Component Test

Of primary concern in this study was the determination of how much cross-polarized E-field component was present in the working volume region of the simulator. It is well known that the configuration of the E-field in a parallel plate guide of infinite extent is something like that which is depicted in Fig. 3.16a. The E-field components of a TEM wave are all parallel to each other and normal to the plates of the guide. For a finite width guide, the E-field components are affected

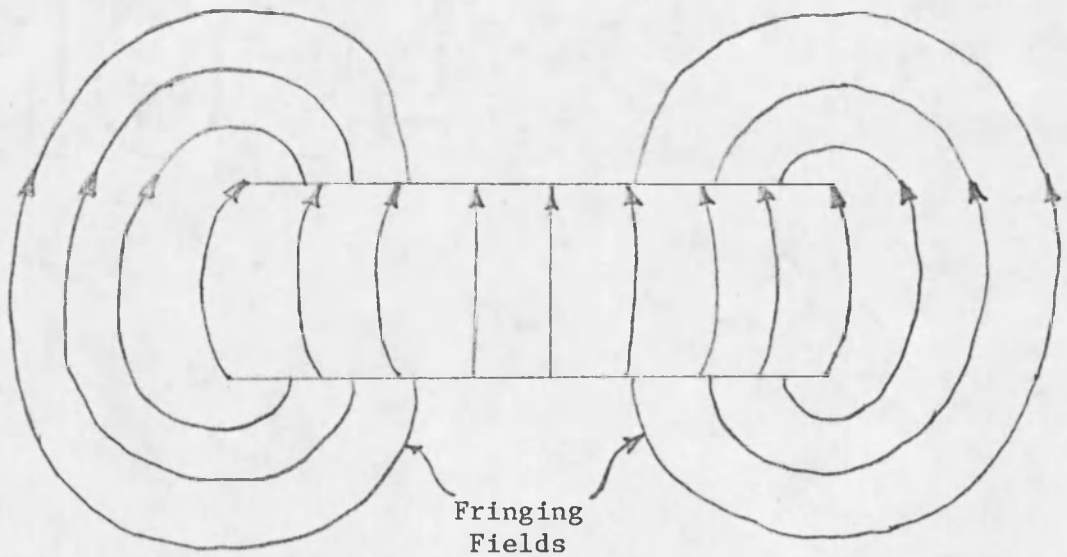


Vertical = .1/Div

Fig. 3.15 Reflection Coefficient for Twin Lead to TEM Horn Connection



(a) Infinite Plate



(b) Finite Plate

Fig. 3.16 E-Field Configurations for Parallel Plate Guides

by the edges of the guide and will look something like those depicted in Fig. 3.16b. The important point to note here is that there are some fringing fields produced around a finite parallel plate structure. The configuration of the E-field components is complicated even further if a ground plane is introduced into the region near the parallel plate guide. This condition is depicted in Fig. 3.17 and essentially represents the condition that exists in the design for the EMP simulator. The E-field components of the wave must satisfy the boundary condition at the surface of the ground plane, which is that the tangential E-field at the surface of a perfect conductor must be zero. Thus, the E-field is bent until it is normal to the ground plane at its point of intersection. This component of the E-field is now cross-polarized with respect to the E-field components contained within the parallel plate structure. Some of this cross-polarized E-field is reflected from the ground plane into the region between the parallel plates which contains the working volume. The measurement of the amount of this field component, as compared to the amount of horizontal E-field present in the incident wave, was of primary importance. To make this measurement, it was necessary to compare the peak amplitudes of the incident E-field which is horizontally polarized, with that of the vertical E-field at various points within the working volume. From Fig. 3.6, test points 4,5,6,7 and 8 are within the working volume and are the points used for this test. The same probe was used to make all measurements to eliminate the possibility of errors being introduced by differences in probes. Also, since only one probe was used, possible interactions between probes were eliminated. The incident E-field was measured at test point 1.

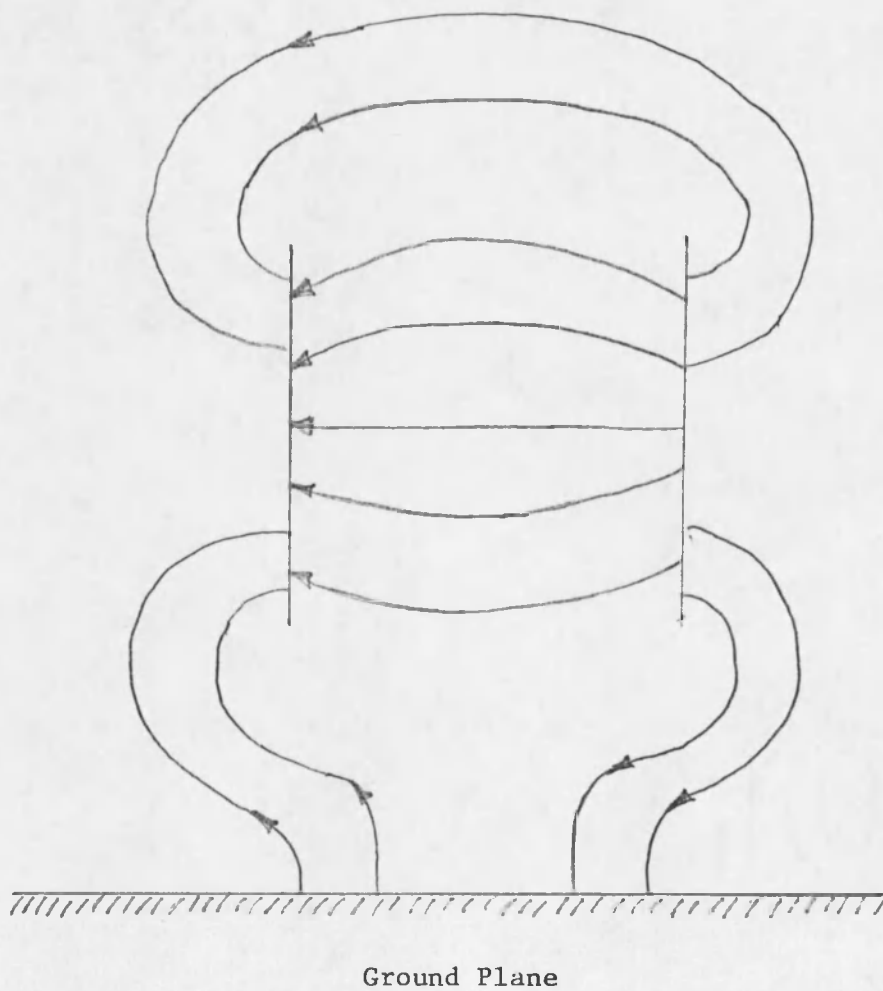


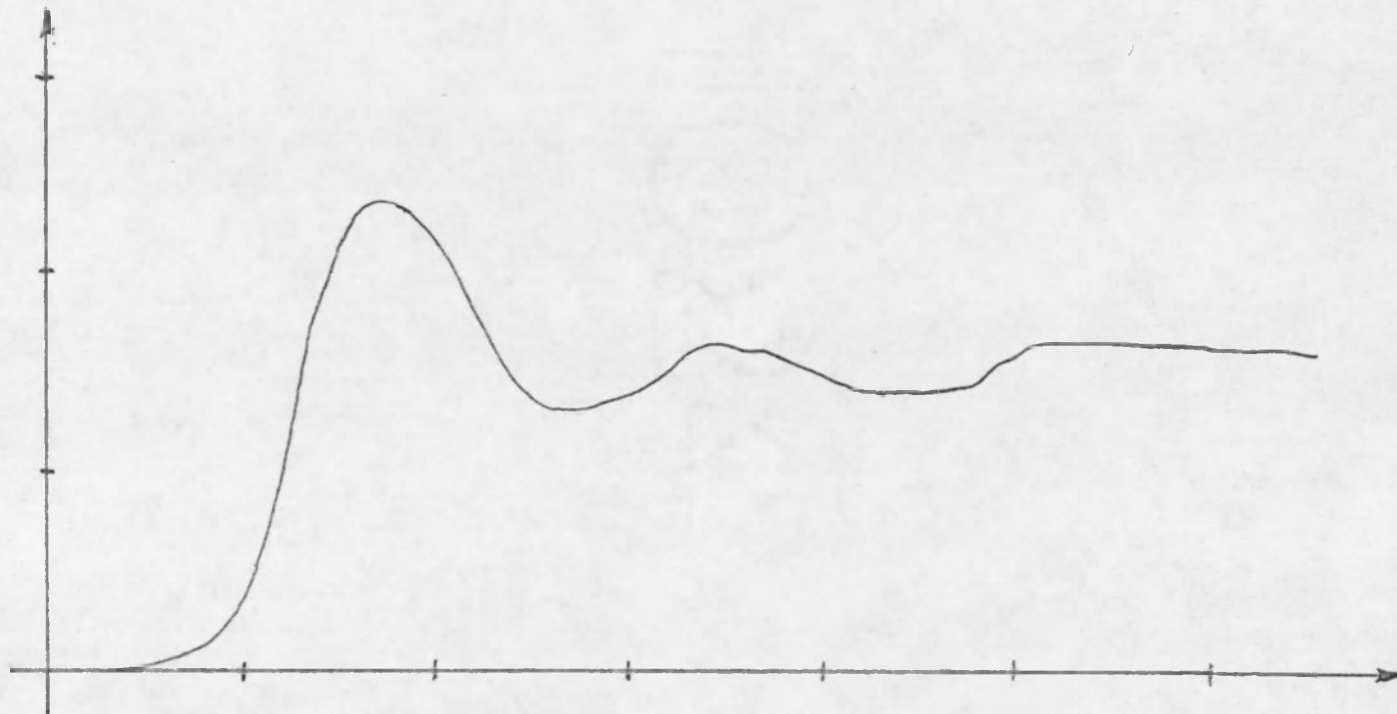
Fig. 3.17 E-Field Configuration for a Finite Parallel Plate Structure in the Vicinity of a Ground Plane

The results of this test indicate that the peak amplitude of the cross-polarized E-field was $1/6$ to $1/4$ that of the incident E-field. Some of the data used for this analysis is shown in Figures 3.18, 3.19, and 3.20. Figure 3.18 represents the incident E-field. It is important to note that these data were attenuated by 10 db. Thus, the actual amplitude is 3.16 times that which is indicated in the figure. The other two figures represent the cross-polarized E-field at test points 4 and 6 in the working volume. The amount of cross-polarized E-field present in the working volume was considered significant in that it could drastically affect any measurements made on test objects in the working volume.

A point of interest is that a parallel study was performed by the University of Mississippi [Dudley, 1974] from a theoretical viewpoint. This study predicted cross-polarized E-field components of the same order of magnitude as was observed experimentally.

Performance Evaluation

With the exception of the amount of cross-polarized component of the E-field in the working volume, the simulator appeared to be producing the desired output. However, its usefulness as a simulator is greatly reduced because the measurements made in the working volume could not be considered reliable enough to be valid. Further study of the design is warranted to determine if it is possible to reduce the amount of cross-polarized E-field to an acceptable level. A more comprehensive mapping of the fields within and around the structure would be necessary to provide a more complete evaluation of the simulator.



Vertical = 200 MV/Div (10 db attn.)
Horizontal = 1 NS/Div

Fig. 3.18 Integrated Response of E-Field Sensor at Test Point #1

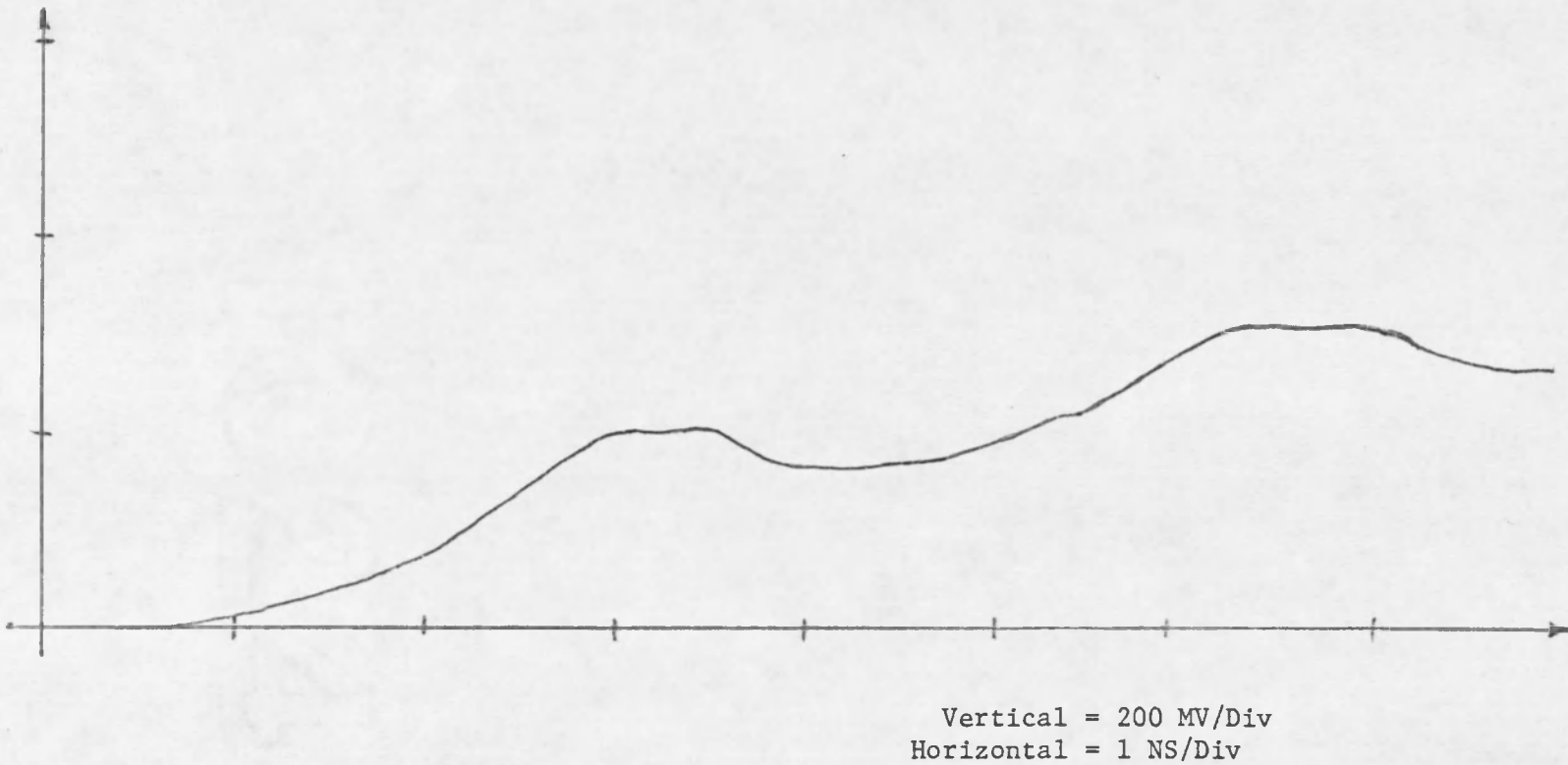


Fig. 3.19 Integrated Response of E-Field Sensor at Test Point #4

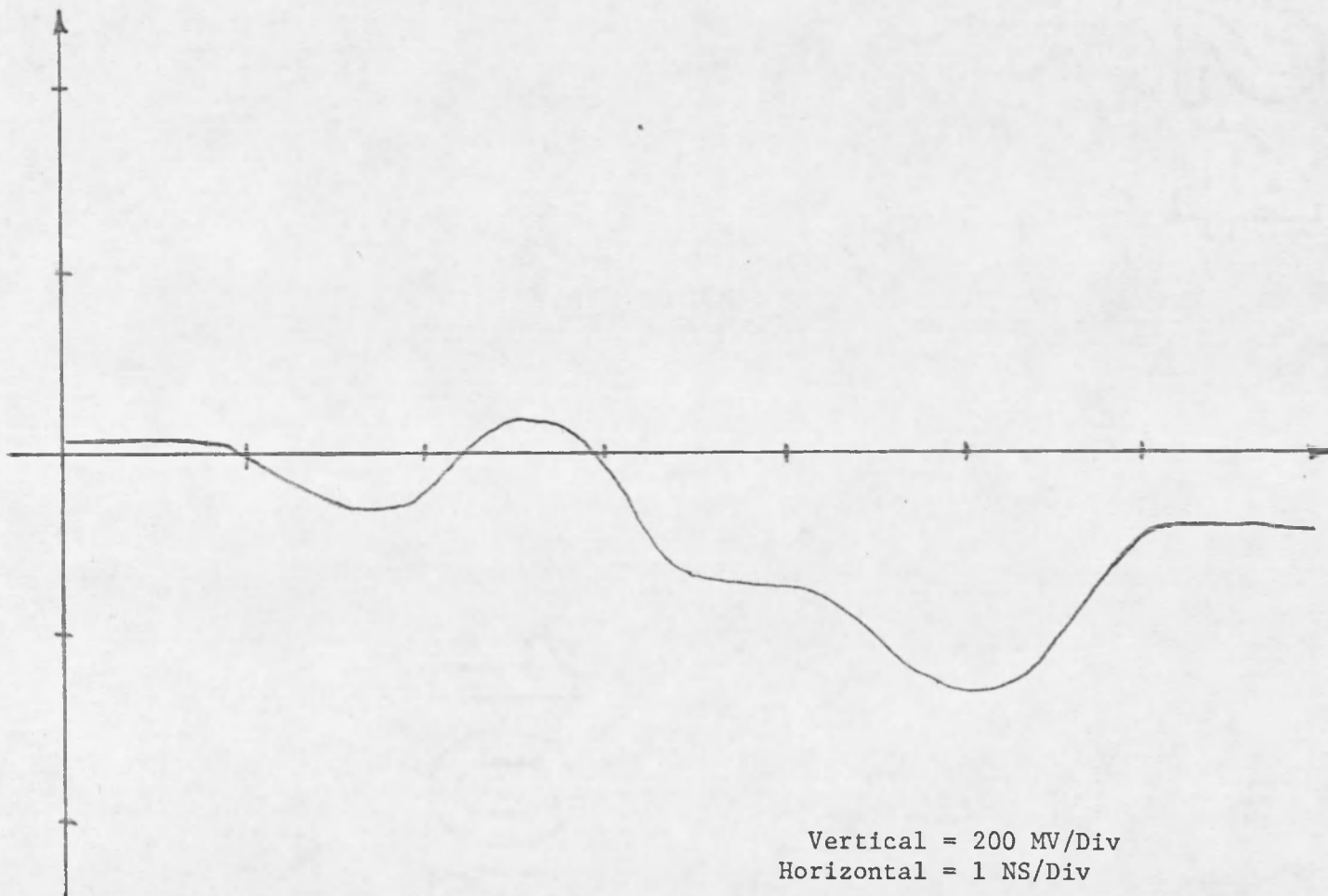


Fig. 3.20 Integrated Response of E-Field Sensor at Test Point #6

CHAPTER 4

CONCLUSIONS

The results of these two studies indicate that the principles of scale modeling can be applied to devices such as EMP simulators as well as they can to other items such as antennas. The value of scale model simulators can be seen when one considers the costs involved in building a full scale simulator or of having to make measurements only during a nuclear explosion. If the design of a full scale simulator turns out to be faulty, the man hours and material expended in its construction would be almost totally lost. Likewise, making measurements during a nuclear explosion is a one-shot affair which cannot be easily repeated and may sometimes result in the destruction of some of the measurement equipment. Therefore, the scale model EMP simulator is an important tool in the study of electromagnetics.

LIST OF REFERENCES

- Dudley, D. G. "EMP Facility Pulse Arrival Angle and Reflection Analysis," Interim Report, Engineering Experiment Station, College of Engineering, University of Arizona, Tucson, Arizona, 14 June 1974.
- Dudley, D. G., and E. F. Oberst. "Electromagnetic Wave Impinging on an Idealized Station," Special Report, Engineering Experiment Station, College of Engineering, University of Arizona, Tucson, Arizona, 28 March 1974.
- E-H Research Laboratories, Inc. Fast Pulse Techniques, E-H Laboratories, Inc., Oakland, Calif., Feb. 1968.
- Schmitt, H. J., C. W. Harrison, Jr., and C. S. Williams, Jr. "Calculated and Experimental Response of Thin Cylindrical Antennas to Pulse Excitation," IEEE Transactions on Antennas and Propagation, Vol. AP-14, No. 2, March 1966.
- Weeks, W. L. Antenna Engineering, McGraw-Hill Book Co., New York, New York, 1968.

